Title
PORE SIZE DISTRIBUTION DURING COMPACTION AND EARLY STAGE SINTERING OF Si3N4

Author
Naito, N.

Publication Date
1985-08-01

LBL-20155

PORE SIZE DISTRIBUTION DURING COMPACTION AND EARLY STAGE SINTERING OF Si_3N_4

N. Naito
(M.S. Thesis)

August 1985

Lawrence Berkeley Laboratory
University of California
Berkeley, California 94720

Prepared for the U.S. Department of Energy
under Contract DE-AC03-76SF00098

Center for Advanced Materials

DISCLAIMER

LBL-20155

PORE SIZE DISTRIBUTION DURING COMPACTION AND EARLY STAGE SINTERING OF Si_3N_4

Naomi Naito
M. S. Thesis

Material and Molecular Research Division
Lawrence Berkeley Laboratory
and
Department of Materials Science and Mineral Engineering
University of California
Berkeley, California 94720

This work was supported by the Division of Materials Sciences, Office of Basic Energy Sciences, U.S. Department of Energy, under Contract No. DE-AC03-76F00098.

PORE SIZE DISTRIBUTION DURING COMPACTION AND EARLY STAGE SINTERING OF Si_3N_4

Table of Contents

PORE SIZE DISTRIBUTION DURING COMPACTION AND EARLY STAGE SINTERING OF Si_3N_4

Naomi Naito
Material and Molecular Research Division
Lawrence Berkeley Laboratory
and
Department of Material Science and Mineral Engineering
University of California
Berkeley, California 94720

ABSTRACT

Ceramics based on Si_3N_4, if fully dense with controlled phases and microstructure, are capable of withstanding high temperatures, high stress and corrosive environments. Due to the increasing demand of these materials, processing of ceramics by green body manipulation has been investigated extensively. It is usually found that flaws such as the large cavities which may arise from non-uniform pore size distribution, grow and coalesce during sintering. These circumstances lead to isolated pores and exaggerated grain growth in the final product: conditions which are known to initiate failure. The present work is hence devoted to achieving a more uniform pore size distribution for Si_3N_4 powders during compaction and early stage sintering.

Some of the parameters that affect the structure of the green compact during die compaction are load, compaction rate, lubricant/binder characteristics and compact viscosity and relaxation behavior. Relationships of these parameters to pore size distribution were obtained. Specifically, a correlation was made with three predominant elements of the pore size distribution curves: the mean pore radius, the dis-

tribution around the mean pore radius and the existence of "tails" in the distribution curves which indicates the presence of larger pores in the powder compact.

A more uniform pore size distribution curve was obtained through the use of viscous polymer binders. Powder rearrangement was promoted following compaction, by stress relaxation. Furthermore, there seemed to exist an optimal viscosity level for the polymer binder, a compromise between a narrow pore size distribution around the mean pore radius and a reduction in the number of larger pores.

During the early stages sintering of the Si_3N_4 with Y_2O_3, a high percentage of transformation and minimal densification were observed; yet uniform green structures were maintained.

ACKNOWLEDGEMENTS

I would like to express my deep appreciation to Professor Lutgard De Jonghe and Dr. Len Rahaman for their excellent guidance and support in this work. I would also like to thank Professors Alan Searcy and K. V. S. Sastry for critical reading and comment on the thesis.

Interactions with colleagues and friends greatly assisted the completion of this work. Special thanks to Dr. Chun-Hway Hsueh for theoretical assistance, Yves Boiteux for helpful discussions, Dale Olson for text editing, Martin Weiser for help in the computer work, John Holthuis for his furnace, and to the very helpful secretary, Raquel Rodriguez.

1. INTRODUCTION

Ceramics based on Si_3N_4 and the phases of the SIALON system(s) are of considerable interest as high temperature engineering materials. Dense Si_3N_4 exhibits high strength and wear resistance, high decomposition temperature, oxidation resistance, excellent thermal shock resistance up to 1400°C, a low coefficient of friction and resistance to corrosive environments (Ka84a, Po84). These ceramics have important future applications, such as in tooling, in space shuttles, or in automobiles. Materials in these environments are exposed to high temperatures and stresses, compounded by shocks and vibrations (La84c, Ri81).

Fabrication of suitable ceramic parts depends on the characteristics of the green powder compact. Flaws, usually in the form of chemical or structural inhomogeneities, may be introduced during the preparation of the green compacts (Po61). They originate from lamination during die pressing, introduction of hollow agglomerates found in some spray dried powders, binder accumulation or incomplete burnout, inclusion of foreign materials, or any number of other processing variables. The firing process usually amplifies the defects, lowering the sintering rate and the final density of the ceramic (Br82, Cu78, Ro81).

A major consequence of improper processing is the existence of isolated pores within the grains of the final sintered products. These pores can only be eliminated by the much slower mechanism of lattice diffusion. In this case, shrinkage is negligible (Hs82,

Bo66), and full density practically can not be achieved (Wi83). Additionally, further sintering may induce exaggerated grain growth, which in turn degrades the mechanical properties of the products.

To avert the isolation of pores during sintering, many researchers (Fr84, Br82) have focused on process variables such as additives, atmosphere, particle size and size distribution. For example, small size and narrow particle distribution generally are believed to yield high densities through homogenization and decrease in pore size. Thus, by preventing the ultimate growth of the pores reaching the critical pore-grain boundary separation region, higher density can be achieved (Hs82).

The intent of this work was to develop a method to increase the homogeneity of the green compact through improvement in the pore size distribution. A polymer solution serving as a lubricant, was mixed with the silicon nitride powder. The mixture was pressed wet in a die and excess lubricant was drained and load stress was relaxed. The powder rearrangement effects during the one-side die compaction were studied through pore size distribution characteristics measured by mercury porosimetry. Effects of relaxation, compaction rate, load and compact viscosity were also studied.

The compacts were sintered for short times to study the effects of rearrangement and phase transformations during the initial stage of sintering.

2. SILICON NITRIDE

2.1 Powder

For the sintered or HIP-ed (Hot Isostatically Pressed) silicon nitride to compete with the traditional methods of RBSN (Reaction Bonded Silicon Nitride), the availability and the cost of high quality silicon nitride powder become important issues. The increasing abundance of the commercial powders from GTE in the U. S., H. C. Starck in Germany and Toshiba in Japan has been a major thrust in the development of sintered silicon nitride.

Starck (Sc84) utilizes the most direct and common method of silicon nitride formation through nitridation of the silicon powder:

$$3Si(s) + 2N_2(g) = Si_3N_4(s) \qquad (1)$$

The powder produced below 1450°C is predominantly alpha phase (see section 2.3.2). However, the current synthesis by nitridation usually requires a catalyst, involves in vapor phase reaction, and forms strong agglomeration which requires attrition to reduce the powder size (La84a,d).

The carbothermic reduction of silica followed by nitridation is considered desirable by Toshiba (Mo84a, Ko83) due to the wide availability of pure and fine powders of silica and carbon. The reaction is:

$$3SiO_2(s) + 6C(s) + 2N_2(g) = Si_3N_4(g) + 6CO(g) \qquad (2)$$

Large surface area and high alpha phase silicon nitride can be produced directly through the above reaction. The excess carbon is used as an oxygen sink, by forming CO, to minimize oxygen on the surface of Si_3N_4. The oxygen, which forms silica, contributes to liquid phase sintering by forming a viscous glassy phase. The amount and properties of this phase must be controlled to achieve the required mechanical strength.

Vapor phase reaction of gaseous silicon compounds such as silicon tetrachloride or silane with ammonia leads to the following reaction utilized by GTE (Bu78, Ma73):

$$3SiCl_4(g) + 4NH_3(g) = Si_3N_4(s) + 12HCl(g) \quad (3)$$

$$3SiH_4(g) + 4NH_3(g) = Si_3N_4(s) + 6H_2(g) \quad (4)$$

Through these reactions, very fine amorphous silicon nitride possessing high purity (with the exception of hydrogen) can be produced. However, corrosion problems exist with the use of $SiCl_4$, and SiH_4 is expensive. Some of the amorphous phase is converted to alpha phase during calcination, conducted for purification purposes following the powder formation (GTE SN502 grade powder used for the present study). The calcined powder has low packing density with large volume of needlelike alpha structure. Table I provides a comparison of five Si_3N_4 powders prepared by the three methods.

The imposed powder preparation routes may introduce considerable variations in the properties of the powders such as phase content,

surface area, or purity. Consequently, further improvement of the commercially available powders awaits extensive research (Sz81, Wi83b, Jo81). Efforts in the research of laser heated gases for molecular excitation and reaction (Mo83), as well as reaction of compound gaseous silicon-nitrogen compounds in organosilicon materials powders, is being pursued (Jo81, Ya83).

Effective sintering places stringent demands on the starting material characteristics. Alleviating the possible future processing and sintering complications requires the incorporation of the following characteristics of the starting silicon nitride powders (Ka84a, La81b, Ro81, Po61):

(1) High specific surface area. The small particle size increases the thermodynamic driving force for sintering as well as reducing diffusion distances and thus the sintering time.

(2) High alpha phase content. Starting powders with small volume fractions of beta phase have been found to inhibit the alpha to beta transformation (La84a, Me78). Maximum strength of Si_3N_4 is reached at nearly full conversion of alpha to beta phase with interlocking, elongated grains with high aspect ratios. The more pronounced fibrous structure of the beta phase augments the strength and fracture toughness of Si_3N_4. Any further sintering will coarsen the beta grains and only leads to lower strength of the material (sec. 2.3.2).

(3) Low metallic and carbon contamination. The incidence of metallic contamination commonly reported to date (Ca, Al, Fe, Na) (Pa84b, Cl82, Gr78, Ri73) forms metallic inclusions resulting in identifiable fracture origins. Inclusions such as Fe have also been shown to increase the oxidation rates of silicon nitride (Pa84b). Carbon contamination leads to the formation of SiC which resides in secondary crystalline phases (Cl81). These particles degrade the mechanical strength of the ceramic by acting as origins for cracks.

(4) Controlled O_2 and non-metallic content. The SiO_2 content of Si_3N_4 is critical to the densification and formation of liquid phases which enhance the transport of Si or N (Bo85, Gr80, Kr79, Sc77). Non-metallic elements in Si_3N_4 such as chlorine can remain in hot-pressed compacts up to 1750°C, inhibit reactive hot pressing and stabilize the alpha phase (Cl82).

(5) Good Compactibility. Compactibility is related to individual powder characteristics such as hardness, agglomeration and morphology (Lu78, Dy83). Hard agglomerates typically contain strong chemical bridges between the particles, whereas soft agglomerates are connected through less permanent bridges such as van der Waals type bonds (La84a, Ni78). The presence of hard agglomerates and whisker morphology lead to low green compact density.

2.2 Process: Green Compact formation

Several processing methods have evolved including injection molding (Ba85,Ma83, Mo83), sol-gel processing (Sz81, He84), slip casting (Fe72, Wi83, Gu84, Ma84) as well as traditional compaction methods such as die-compaction with binder modifications, lubricant addition, freeze drying (Pa83) and spray drying (Si82, Lu78). The universal objective underlying these studies is the control of the packing characteristics of ceramic powders in the final mix formulations. In this regard, however, very few scientifically based guidelines have evolved (La81b).

The traditional processing cycle (specifically for Si_3N_4) constitutes the following. Treatments such as calcination aimed at improving the quality of the available Si_3N_4 powder, followed by mixing (Ro70) the oxide additives (e.g., Al_2O_3, MgO, Y_2O_3 or combinations of additives for SIALONS) as sintering aids for densification. The material is then milled. Researchers at Air Research (Dr81) investigating injection molding of Si_3N_4 showed a significant improvement in dry compaction density with powder ball milling for 24 hours. This improvement was attributed to the breakage of fibrous Si_3N_4 needles and the subsequent reduction of average aspect ratios.

In general, materials with a whisker morphology are milled to achieve higher packing densities. However, the ball milling procedure often leads to agglomeration and non-uniform packing densities as well as to metallic contamination from the milling balls (Dy83, La84a,b, Lu78). For processes such as attrition milling, subsequent chemical

treatments are necessary to remove metallic impurities (e.g., Fe). Recent developments in impact milling involve air classification with high velocity air streams constantly impinging on the particles. Combined with gravitational force, this allows for the separation of the milled particles and thus reduces agglomeration.

In conjunction with the ball milling, the additives and compaction aids can be mixed efficiently with Si_3N_4 powder in a planetary mill. A uniform distribution of small amounts of additives and compaction aids can be also achieved by spray drying, if the additives are used in solution form (Si82, Lu78).

For methods such as injection molding, it is essential to tailor the initial particle size distribution of the powder (Ma83). The process of injection molding of ceramics as outlined by Schwartzwalder (Sc49) proposes mixing of a ceramic powder with an organic binder (either thermoplastic or thermosetting). The mixture is injected into a die cavity. The part is removed from the cavity and the binder is removed through a low-temperature heat treatment. This green ceramic shape can then be processed using the normal ceramic molds. It is important that the green density of the injection molded articles is high in order to minimize firing shrinkage, because the main application of injection molding is for the fabrication of large quantities of complex shaped ceramic articles with high dimensional tolerance.

A high solid concentration (Fa68) in the injection-molded material must be balanced with a viscosity low enough for the molding process. Studies report that the incorporation of increased solids concentration with a broad rather than a narrow particle size distribution does not

increase the viscosity of the system or alter the rheology of the mixture (Fa68, Ma83).

2.3 Sintering

The basic objective for sintering is to obtain ceramic materials with high density, controlled grain size and amount and distribution of any secondary phase. Significant densification results only from transport mechanisms which decrease the distance between centers of particles during initial stage sintering. There are several transport paths, but only two mechanisms - which involve grain boundary and lattice diffusions (dislocations) - exhibit this characteristics. Alternately, arrival of matter from the free surface of the particles (surface diffusion) or material transport through the vapor phase (evaporation/condensation) lead merely to neck growth and microstructural coarsening without any appreciable densification (Gu72, Kn84). Unfortunately, due to the covalent bond nature of Si_3N_4 (70% covalency for Si-N) high activation energy is necessary for the formation and motion of the structural defects which permit densification by diffusion (As74, Gr77).

The predominant techniques for the densification of Si_3N_4 involve sintering, hot pressing or hot isostatic pressing (Gr84, Gr81a, Ga74, Ga79, La84b, So84, Ye79, La82). However, there is a upper limit to the sintering temperature for Si_3N_4 because of the appreciable partial pressures of silicon and nitrogen. High temperature sintering (~1600°C) of pure Si_3N_4 leads to massive loss of material, with decomposition

accompanied by an increase in surface area. High N_2 pressure as well as protective Si_3N_4 powder beds (Po81, Wo84) must be used to minimize the weight loss.

Hot pressing has been used most extensively for densifying Si_3N_4 (Ga79, Ga74, Te74). It is performed at very high pressures (up to 500 MPa) thus decreasing allowable sintering temperatures to nearly 1700°C.

Pressureless sintering has the inherent advantage because of low cost and flexibility involved in formation of complex shapes. Important developments in the last decade have been devoted to understanding and inhibiting thermal decomposition while improving densification rates such that pressureless sintering has yielded mechanically acceptable parts (Ka84a,b, Po84, Od78).

The densification of Si_3N_4 by either hot pressing or pressureless sintering requires an additive which reacts with the surface silica and some of the nitrides. This gives an oxynitride liquid that simultaneously promotes shrinkage, and the phase transformation from alpha to beta.

2.3.1 Liquid Phase Sintering using Sintering Aids

Various compounds (Y_2O_3, MgO, BeO, CeO, ZrO_2, Sc_2O_3, Mg_3N_2, La_2O_3, $BeSiN_2$, or SiO_2) have been used singly or in combination in various concentrations to promote densification. The metal oxide additives form a liquid phase with surface silica (Gr81b, Bo78) leading to glassy or crystalline oxynitride boundary phases which influence the microstructure and mechanical properties of Si_3N_4.

The diversity in the effects (mechanical properties, sintering rates etc.,) of the various additives is critically related to the amount and properties of the liquid phase formed at high temperatures (Ja84, Le83, Lo80). Kingery (Ki59), in his theoretical treatment, discerns three possibly overlapping stages of liquid phase sintering:

Stage I. Particle rearrangement, immediately following the formation of the liquid phase, is brought about by the remaining solid particles sliding over each other under the action of capillary forces. The rate and extent of shrinkage will depend on the viscosity and quantity of the liquid and its wetting properties.

Stage II. A solution-reprecipitation process will be dominant if the solid particles have some solubility in the liquid phase. Since the solubility at the contact points of solid particles is greater then the solubility of solid surfaces, material transport away from the contact points will allow the densification. The volume change resulting from this can be described by

$$\Delta V/V \propto t^{1/n} \qquad (5)$$

where n=3 when the rate controlling process is solution- precipitation from the liquid, and n=5 for diffusion control.

Stage III. This stage, described as coalescence or isolated pore elimination, requires solid state diffusion. However, shrinkage due to this is unlikely in the case of silicon nitride, unless very high pressures are used.

Hampshire and Jack (Ha84) interpreted the densification mechanisms of silicon nitride with the additives MgO and Y_2O_3 by using the Kingery model. During the early sintering stage, rearrangement and densification of Si_3N_4 depend critically on the viscosity of the silicate melt. Due to the lower viscosity of the MgO melt, its contribution to densification is larger than that of Y_2O_3 with minimal transformation from alpha to beta phase. For MgO, over 90% of theoretical density is achieved with little or no densification during the early stage of sintering. The solution precipitation mechanism of beta phase in contact areas is considered to be the dominant process for Y_2O_3 resulting in no significant material transport. Thus full phase transformation to beta phase is achieved with minimal densification.

Despite the rapid transformations during densification and oxidation problems at intermediate temperatures, Y_2O_3 based Si_3N_4 provides substantial benefits in terms of high temperature mechanical properties compared to MgO based Si_3N_4 (Ka84, Od84, Bi84). This is primarily due to the more vitreous properties of the liquid phase. The ultimate progress in grain boundary engineering (Ka77) for the Si_3N_4 based materials is the achievement of complete crystallization of the glassy phase and the formation of a refractory crystalline phase.

2.3.2 The Alpha to Beta Phase Transformation

The idealized silicon nitride structures can be described as a stacking of Si-N layers in either ABAB... (beta) or ABCD... (alpha) sequence. This gives, in the hexagonal beta unit cell containing

Si_6N_8, long continuous channels running parallel with the c-direction, and centered at 2/3 and 1/3. In alpha, the c-glide plane that relates the layers CD with AB replaces the continuous channels of beta by large, closed interstices at (2/3, 1/3, 3/8) and (1/3, 2/3, 7/8). The actual beta structure is nearly identical to the idealized structure. However, the alpha structures are actually distorted, and the nitrogen atoms at heights approximately 3/8 and 7/8 are pulled towards the centers of the two respective interstices. There is also a wide variation in unit-cell dimensions and density of the alpha phase (Ja84).

The alpha to beta transformation is a reconstructive transformation of second coordination involving the breaking and reforming of Si-N bonds, and requiring either an intermediate vapor phase or a solvent phase (Ha84, Ha81, Me78). The maximum strength of silicon nitride is achieved at the point of full conversion of alpha to beta phase, with an interlocking elongated grain morphology exhibiting high aspect ratios. Any further sintering usually leads to grain coarsening. To prevent rapid conversion of alpha to beta phase, starting powders with high alpha content have been shown to be effective (Kn84, Me78, Bo78b).

The influence of this preexisting beta phase grains on the transformation rate, as well as the influence of enhanced nucleation of beta, may suggest the control of the alpha/beta interface on transformation kinetics. Possible mechanism is suggested by Knoch et.al. (Kn84) for hot pressed Si_3N_4. It is assumed that during the early stages of transformation of the dense body, isolated beta grains are embedded in the alpha matrix.

During the grain growth of beta and phase transformation, there are three possible rate limiting mechanisms; the dissolution of alpha into the liquid, the diffusion through the liquid, and the reprecipitation at the beta surface (Ja84, Kn84). For the initial densification step, both the solution reaction (Kn78) and the diffusion through the liquid (Bo78b, Me78) have been discussed as the rate limiting processes (Cl77, La82). As the material becomes more dense, diffusion distances for solution reprecipitation process become short and the reaction step at the interface of liquid grain boundary phase and beta phase becomes rate controlling. The precipitation step also leads to the growth of the beta phase perpendicular to the c-axis (the slower growing direction) resulting in the equiaxed shape (Kn84).

3. DIE COMPACTION

One-sided die compaction has been an object of extensive study (Fr84, Fi83, Is83, Me82, Br83, La81a, Th81a,b,c, St79, St77). It is one of the most widely used forming operations in the ceramic industry for dry and semi-dry pressing. The desired shape is formed by application of external forces on material loaded into a mold or a chamber (Th81). The packing density is controlled by the applied stress, the constraining forces that the mold wall imposes, and the characteristics of the material. Internal uniformity depend on the uniformity of the stress distribution.

3.1 Die wall friction and density variation

During compaction, the pressure applied to the powder is not transmitted uniformly because of intra-particle friction and friction between the particles and the die wall. To quantify the effect, soil mechanics, a branch of continuum theory which provides a methodology for treating stress and strain distribution within a particular system, has been used extensively.

Schwartz and Weinstein (Sc65) were the first to apply the concept of soil plasticity for compaction of granular materials. The Coulomb yield criterion states that the failure occurs when the shear stress on any plane in the material reaches a critical value. The authors implicitly assumed a rigid plastic model, where plastic irreversible yield occurs at the intersection of Mohrs circle and the yield point (Ti51). However, at least for metal powders (Ca84, St77), the compact behavior at high pressure deviates from this rigid plastic model. There is continuous plastic deformation below the yield point. Thus, there was a shift to analysis of powder failure below the yield stress.

Consistent with the general trend, Stijbos et al. (St78, St77) and Thompson (Th81a,b) analyzed the elastic stresses and strains in die compacted powders. Thompson derived the stresses that caused a distribution of localized green densities, expressed in terms of bulk engineering parameters such as die friction and geometry. The results were used to derive analytically the conditions that cause endcapping. As the ratio of length to diameter of the compact increases, the com-.

pact is subject to more side wall friction. This increased proportion of shear causes increased density variation within the compact.

Strijbos experimentally studied the powder-wall sliding effect by using a metal bar of an unlubricated wall material clamped with a known stress between two disks of powder. The metal bar was moved at a continuous displacement rate and the required force to move the bar was recorded. At some distance, "powder - wall failure" occurred and the friction coefficient reached a constant value.

This value evidently depends on the powder particle hardness, wall hardness and the ratio of particle size and to the roughness of the wall. For nearly smooth walls, failure occurs at the powder-wall interface, whereas for rough walls, powder failure occurs internally.

For fine powders, a "sticky layer" (St77) forms at the die wall leading to high friction, regardless of the hardness of the powder-die interface or the roughness of the wall. The external friction can be reduced by granulating the particles, through methods such as spray forming, thus increasing the size and flowability. For coarser powders friction depends on the powder hardness, die hardness and die roughness. Fracture must occur to fill the small void spaces until very high pressures are reached for plastic flow. Softer particles, due to their plastic flow at relatively lower compaction pressures, gain greater fractional volume compaction at the given pressure. To reduce the die wall friction, the die wall must be harder than the powder and the die wall groove size smaller than the average particle size.

4. LUBRICANTS AND BINDERS

Successful forming of a ceramic part depends on the preparation of moldable raw materials that can produce green bodies with the required characteristics. Thus, it is common practice to prepare the suitable raw materials with combination of additives that aid in the forming process. This is a critical step prior to the consolidation process for methods, such as isostatic pressing, dry pressing, tape casting, extrusion, roll forming, thick film printing, compression molding, semidry pressing and injection molding. The forming additives include a wide range of organic polymers, liquids, plasticizers and dispersants (On85). The resulting mixture is an composite of interacting particles with the additives occupying the voids between the particles.

Of the ceramic processes listed above, all except injection molding and compression molding involve the use of binders that are dissolved or dispersed in liquid. The binders are dissolved molecularly in water or an organic solvent, or are dispersed as a liquid emulsion. The liquid phase is important for uniformly dispersing the binder throughout the particles. It is necessary for providing fluidity to slips or plasticity for extrusion and semidry pressing. Dry green strength in the body is developed by evaporation of the liquid. The binder is retained in the body, and provides organic bridges between the ceramic particles.

Several authors (Ni84a,b, Di84, Di83, Br81) have reported how the binder characteristics can influence the stress transmission of the powder during dry compaction. Use of the binder PVA (poly-vinyl al-

cohol) with different degrees of absorbed moisture (which acts as a plasticizer), or binders with a low glass transition temperature (Tg) resulted in softer granules for alumina powder. The improved deformability of the compact leads to more reproducible pressing and enhanced springback of the compact.

The effect of lubrication depends on the particle size. For small particles, wall roughness is unimportant and friction decreases with increasing lubrication. For coarse powders, however, wall roughness is more important than lubrication (St77).

5. VISCOSITY

As stresses can be relaxed by viscoelastic deformation, materials with lower viscosity can relax stress within the green compact faster. This in turn, possibly results in less intrinsic damage within the material.

For binder selection, the imparted viscosity is one of the primary considerations for a specific process. While the binder is added to provide the necessary green strength, it must also impart the appropriate viscosity to the liquid in the batch material. For slip casting, doctor blading and spray drying, the slip must have a sufficiently low viscosity. In contrast, the liquid present for extrusion processes must have a high viscosity. If the liquid is too fluid, it will be squeezed out and separated from the ceramic material.

The possibility of alleviating the heterogeneity in the green compact through use of viscous flow during compaction has been explored.

The viscosity will influence the particulate system and the compaction behavior. The stress relaxation due to the high temperature induced viscous flow and creep accommodating differential sintering can possibly be of assistance to cold compaction of powder containing a viscous flow medium.

6. EXPERIMENTAL

Reliability and performance of dense silicon nitride can be improved through compositional or microstructural alterations. The compositional approach involves additive selection, and control of impurity effects and phase equilibria. Microstructural improvements rely on starting material characteristics and selection of process parameters. The method implemented in the following study is the microstructural homogenization of powders through rearrangement of grains during relaxation in die compaction. The overall experimental procedure adopted in the present study is outlined in Fig. 1.

6.1 Powder Characteristics

The phases in the as received Si_3N_4 were 40% amorphous and 60% crystalline. The crystalline phase consisted of 91.4% α phase and 8.6% β phase as determined from the X-ray diffractometer analysis (Siemens D500). The surface area of the Si_3N_4 powder was 4 m^2/g, and the grain size of Y_2O_3 powder used as the densification aid was 0.5μm.

6.2 Processing

Silicon nitride and yttria (10:1 weight ratio) were initially mixed dry in a twin shaft dry blender for 24-48 hours and then agitated wet in ethanol with a magnetic stirrer to break-down agglomerates. The wet mixture was then dried in an oven under vacuum for one day at 30°C.

The silicon nitride/yttria powder mix was separated into 0.75g of powder. The powders were compacted under the following conditions;

a. without additives (DRY)

b. with polymer lubrication (POLY)

c. with a binder (BINDER).

The solution of polymer lubricant consisted of different concentrations of polystyrene in chloroform. The amount ranged from 1 gram of polystyrene in 2.5 to 15 cc of chloroform. These mixtures yielded a wide range of viscosities for the particulate system. In addition, powders were coated with an organic binder (carbowax) using a solvent, ether. Carbowax is one of the commonly utilized binder in the industry.

6.3 Compaction

A half-inch one-sided steel die was lubricated with a 2% steric acid-acetone solution. Each type of mixture (powder with polymer, ethanol and binder) as well as the dry powder without any form of lubrication, was cold pressed with an Instron (TT floor model) with and without stress relaxation (Fig. 2). In the non-relaxed mode, the pellets are pressed at a constant strain rate and the load is removed

when the stress reaches a desired point. For the stress relaxation mode, the total strain is kept constant when the desired level of stress is reached. The effects of compaction rate, load, polymer lubrication and the relaxation of the pellets were studied. In all cases, except for the load effect curves, the total strain of the compacts was kept constant to achieve a constant green density.

The effect of the viscosity of the compact on the pore size distribution was studied as follows. The powders were combined with polystyrene-chloroform mixtures of different viscosities. The compacts were pressed to a fixed stress and the stress relaxed (in Instron Model # 1122). The load used in this part of the study was about one-fifth (50 MPa) of that in the previous section. This was done mainly to accentuate the effect of viscosity.

The powder, after initial compaction, was reloaded to a sufficiently low load such that the change in the density, and thus, the elastic modulus, was negligible. The viscosity of the final compact was calculated from the ideal loading curve following an analysis developed by Hsueh (Hs85c). Some of the viscous pellets, after being pressed to the final density, were heated to 130°C (above the glass transition temperature of polystyrene) and reloaded to a low load. Stress relaxation was then recorded and viscosity of the pellets was calculated (Appendix B).

The densities of the green compacts were calculated from the height and the thickness of the samples measured by precision micrometers. The results were confirmed through the cumulative pore volume data from mercury porosimetry.

6.4 Early Stage Sintering

The relaxed dry and polymer lubricated compact were pressed to the density of 1.35 g/cm^3 (200 Mpa and 170 Mpa respectively), and sintered at 1750°C under 1 atmosphere of flowing nitrogen. The pellets were then packed in Si_3N_4 powder beds. When the sintering temperature was reached the furnace was turned off (0 min. hold). Sintering was also done for 10 min. (10 min. hold). The effect of the initial pore size distribution on early stages of sintering was studied.

6.5 Mercury Porosimetry

Continuous-scan Hg Porosimetry (Quantachrome Autoscan 60) was used to obtain total pore volume versus mercury pressure curve. The derivative of the pressure versus volume plots and calculation of Dv (see Appendix A) yield pore size distribution curves (Dv vs. pore radius) (Lo81).

RESULTS

7.1 Pore Size Distribution

The pore size distributions of non-relaxed dry and polymer lubricates compact are shown in Figure 3. The non-relaxed compaction used in this study most closely resembles the procedures employed in the usual one-sided die compaction of cold pressing (Th81). The polymer-

lubricated sample achieved slightly smaller average pore size as well as pore size distribution. These contained a measurable fraction of large pores, although to a lesser degree for the polymer lubricated sample. Both compacts were pressed at a compaction rate of 0.1 cm/min.

The effect of compaction rate on pore size distribution for the polymer-lubricated samples is shown in Figure 4 for the non-relaxed compact. It exemplifies the favorable effects of slower compaction rates during compaction. For the dry compact, higher compaction rates without any relaxation lead to endcapping and other compaction non-uniformities. This results in a green strength too low for Hg extrusion.

Comparison of relaxed and non-relaxed polymer-lubricated compact shows almost identical pore distribution curves (Fig. 5). However, the critical feature of the relaxed curve is the extensive reduction in the volume of larger pores. Comparison between the relaxed and non-relaxed dry compacts (Fig. 6) yielded identical conclusions: that relaxation preferentially eliminated larger pores.

The influence of compaction load on green compact uniformity has been examined by numerous authors (Fi83, Is83, He61). It is generally proposed that increasing load beyond the break-point load (see section 8.1.1) will decrease the median pore size. Figure 7 shows the effect of increasing load on the pore size and distribution for the dry compaction process. As previously analyzed, the medium size pores decreased with the increasing load. A novel and pertinent trend, however, is the improvement in the width of the pore distribution in the vicinity of each peak. Both the peak value and the width of pore

distribution curve around the average pore radius have sharpened with increasing load, although there was no significant decrease in the volume of large pores. These trends indicate that the increased compaction pressure for the dry relaxed powder did not suffice in breaking down the significant amounts of agglomeration.

Pore size distributions of binder (carbowax) coated powder, compacted without relaxation, and dry compacts is shown in Fig. 8. The dry compacts were pressed with and without stress relaxation. The pore size distribution of the binder lies between that of the relaxed and non-relaxed dry compacts for the medium pore radius, distribution characteristics, and the larger pores characterized by long "tail" in the pore size distribution curves.

Comparison of the pore size distribution of the relaxed dry and the polymer lubricated green compact substantiates the effectiveness of the lubricant (Fig. 9). The positive trends are the higher and narrower pore distributions, as well as the diminishing volume of larger pores for the polymer lubricated powder compared to that of the dry compact.

7.2 Viscosity Measurements

The role of viscosity and the relaxation effect may elucidate the particle rearrangement process postulated. Summary of the viscosity measurements of the green compacts is given in Table II. The calculated viscosity (Appendix B) of the final compact increases with increasing viscosity of the initial powder mixture utilized for each

consolidation. The pertinence of the viscosity to the pore distribution is shown in figure 10. The distribution curve indicates a practical compromise between a narrow pore distribution and elimination of larger pores. As the viscosity increases, the fraction of larger pores decrease while broadening the pore distribution curve. The larger volume of pores exist for these polymer lubricated samples due to the low load utilized during the compaction, possibly not being beyond the break-point pressure.

The significance of heat treatment of the compact is evidenced in figure 11. Through holding a low load and heating to temperature above the glass transition temperature of the polystyrene, the improvement in pore size distribution is accentuated.

7.3 Sintered Compacts

Finally it is instructive to examine the consequence of the compaction cycle on sintering. Figures 12 and 13 show the effect of early stage sintering on dry and polymer lubricated compact, respectively. Significant phase transformation of the alpha to beta grains occurs in this short time duration, namely from 17% at 0 min. hold to 92% at 10 min. hold. Comparison of the dry and polymer lubricated compact (Fig. 14) shows the prevailing influence of the superior green structure onto the pore distribution of the sintered compacts.

8. DISCUSSIONS

8.1 Green Compacts

The implications of the effect of the parameters discussed in the preceding section, on the green compact homogeneity will be examined, and related to the pore size distribution.

8.1.1 Effects of load

Pressure-density curves relation are frequently studied for the compaction response of metal (Ca84, He61, Ja72) and ceramic powders (Me82, Br66, Lu78, Le70) and a rigorous mechanistic approach is possible. When pressed ceramic density is plotted against logarithm of pressing pressure, a linear relationship is often observed. A "Break Point" may be defined as a existence of a break on a pressure-density curve and can be attributed to the fracture or deformation of agglomerates. With sufficient pressure agglomerates may possibly be eliminated.

Pressure-density relation can be a systematic tool for quantifying the green compaction cycle in terms of experimental parameters such as pressing rate, powder characteristics or fill rates. To further understand the compaction phenomena, a tractable microstructural approach to compaction is presented here with the pressure versus pore size distribution curves.

As previously reported the pore size decreases with the increase in load. However, enhancement of the distribution with increasing load of dry compacted powder has not been discussed. For a dry compacted Si_3N_4, relaxed, the distribution of larger pores did not change appreciably with the increasing load. This possibly indicates that there is no significant agglomerate breakdown. A subsequent section will postulate that the lack of viscous flow in the dry compacts inhibits the destruction of the agglomerates.

8.1.2 Effect of Compaction Rate

The enhancement of the pore size distribution for the polymer lubricated compact, both relaxed and non-relaxed, is apparent in figures 8 and 14. In all cases, the compaction rates employed were 0.1 cm/min. At a compaction rate greater than 0.1 cm/min, dry compacts, in both relaxed and non-relaxed modes, showed severe endcapping and green strength too weak for Hg extrusion. During compaction, the dry compact undergoes a non-reversible density increase (plastic) through high shear and compressive strains. When the ram is withdrawn, the material is abruptly relaxed through elastic springback. Depending upon green compact characteristics, varying degrees of elastic springback are possible. However, when the allowable springback exceeds the elastic limit, cracking results. For one-sided die compaction with rigid die walls, various shear and tensile stresses occur as the ram withdraws.

Allowing slower compaction rates seems to have resulted in lowering these shear and tensile stresses at the ram because rearrangement in the powder relaxes stress. This can be seen from the increasing green strength correlated with progressive rearrangement as evidenced by the improvement in the pore size distribution from dry compact/non-relaxed, to dry compact/relaxed, to polymer lubricant/non-relaxed and to polymer lubricated/relaxed.

8.1.3 Effects of Lubricant

The enhanced stress relaxation capability from the polymer lubrication resulted in a superior pore size distribution without any adverse effects of non-uniform stress distributions that lead to end-capping. The lubrication, which increases the powder flowability, possibly extends the allowable elastic springback during the ram withdrawal, thus preventing cracking at higher compaction rates than that possible with dry compacts. In addition, a significant improvement is seen in the substantial elimination of the larger pores evident as the long "tail" in the distribution curves. This long "tail" in the pore size distribution curve was not alleviated with increasing load for dry relaxed compacts (section 8.1.1). Larger pores are detrimental, as their sintering rate is very slow, which in turn results in isolated pores within the grains during sintering and thus lowers the mechanical strength and the density of the final product.

8.1.4 Effects of Viscosity

In order to achieve uniform green compacts, it is essential that the one sided die compaction transmits pressure uniformly to the powder. However, due to the die wall confinement, die wall friction and characteristics of the powder itself, the resultant compact may contain considerable density gradients.

Recently, several authors have mentioned the effect of powder treatments, more specifically, of manipulating certain binder characteristics, such as Tg or moisture absorption of the organic binder, to improve the pressing behavior (Ni84a,b, Di84). The underlying theme in the use of forming additives for the one sided die compaction is the improvement in the powder flowability, decrease in powder friction and increase in the agglomerate break down. Density gradients need to be avoided since they lead to differential shrinkage, and hence, damage, during sintering.

The effect of viscosity of the compacts confirms this conclusion. The mean pore radius remained consistent with the change in viscosity. The lower viscosity powder/polymer system exhibited a narrower distribution around the mean pore radius, due to the increased flow allowing increased rearrangement.

The decrease in viscosity, however, increased the volume of the larger pores, signifying the existence of increased agglomeration. The higher viscosity was more effective in eliminating agglomeration. The lower viscosity, in general, transmits the stress field from

compaction more uniformly resulting in a sharper pore size distribution around the mean radius.

In order to simulate the large pores in the compact, a hollow sphere model was adopted (Hs85, Ki82), in which a spherical pore with radius, a, is surrounded by a fully dense matrix with outer radius, b. The viscoelastic behavior of the system was assessed by adopting the usual assumption that the deformation satisfies a Maxwell model, such that under a constant stress, σ, the stress and strain rate, $\dot{\varepsilon}$, are related by (Hs85a)

$$\sigma = \frac{4(1-f)G\eta\dot{\varepsilon}}{fG + 3\eta\dot{\varepsilon}} \tag{6}$$

where $f = (a^3/b^3)$ is the volume fraction of pore, G and υ are the shear modulus and viscosity of the matrix, respectively. It can be derived from eqn. (6) that, higher stresses are needed for higher viscosity materials to reach the same strain rate. Furthermore, the radial and hoop stresses, σ_r, and σ_θ, at the pore surface can be derived as (Ti51):

$$\sigma_r = 0$$

$$\sigma_\theta = \frac{\sigma b^3}{2(b^3-a^3)} \tag{7}$$

which in turn yield the maximum shear stress, τ, such that

$$\tau = \frac{\sigma b^3}{4(b^3-a^3)} \tag{8}$$

Hence, higher shear stress exists in the higher viscosity materials, which in turn yield a higher probability for the agglomerate break-down during compaction. Thus, there is a viscosity level where-

by a practical compromise between a narrow distribution of pore size around the mean radius and reduction in the existence of the "tail" of the large pores occur.

The compaction behavior of metal powder has been studied extensively (Ca84, He61, Ja72). For the analyses, elastic-plastic behavior of the materials was assumed and constant applied stresses were used to derive the stress-density relation. However, for the present study, the ceramic powder was mixed with a viscous polymer lubricant. Thus, viscoelastic behavior is assumed for the particulate system. In addition, constant strain rates were used. The stress/strain rate/density relation derived in (Appendix C) is

$$\frac{\sigma}{\eta\dot{\varepsilon}} = 1 - \left(\frac{\rho}{\rho_0}\right) \frac{G}{3\eta\dot{\varepsilon}} \qquad (9)$$

8.2 Stress Relaxation during Compaction

For compaction with stress relaxation, the strain is kept constant when the desired pressure is reached. The load is allowed to relax viscoelastically until it reaches a near constant value. The improved pore size distribution of relaxed compact may be attributed again to the attainment of a more uniform stress transmittance within the die compact.

Instead of immediate ram withdrawal and creating tensile and shear stresses at the face of the pellet, the compact is kept under constant compressive strain allowing stress relaxation through rearrangement of the grains. This effect is evidenced in two forms of the pore size

distribution: improvement in the pore size distribution centered around the average pore radius and, more significantly, the marked decrease in the volume of the larger pores. The smaller pores are between the primary particles, while the larger pores are between the agglomerates. Thus, a possible explanation of the reduction of the larger pores with relaxation involves the isostatic breakdown of the agglomeration (agglomeration was inherent in the powder used in the study). The effect is thus more pronounced in the polymer lubricated compact which transmits compaction stress more uniformly than the dry compacts.

8.3 Effect of Early Stage Sintering

The sintering aid, yttria, used in the study promotes increased phase transformation from alpha to beta with negligible densification of silicon nitride (section 2.3.1).

The effect is evidenced upon immediate cooling of the sample after 1750° C is reached (0 min. sintering). The transformed powder fraction is 17%. The increased average pore radius and the deterioration of the distribution curve for both polymer lubricated and dry compact are to be expected as a consequence of sintering.

The concern about the early stage sintering was the microstructural correspondence of pore structure between the green structure and the sintered compact after the abrupt morphological transformation from spherical and needlelike particles to more equiaxed beta grains.

The 92% transformation to the beta phase occurs at 10 min. sintering (1750°C) and results in a considerable increase of the average pore radius and a broadening of the pore distribution curves. However the degree of deterioration is more pronounced for the dry compact which exhibited less uniform pore distribution in the green compact. The superior pore size distribution obtained with the relaxed polymer-lubricated sample is maintained throughout the phase transformation and into the early stage of sintering. Later sintering stages cannot be characterized by mercury porosimetry, but, it is reasonable to conclude that the improvement will persist throughout the densification process.

9. SUMMARY

The significance of green compact homogeneity has been demonstrated in the present study. The basic compact characteristics introduced during consolidation are maintained during the early stages of sintering, and should ultimately influence the reliability of the final product.

The dominant feature of the analysis is the achievement of more uniform green compacts with a commercially available powder, through improvement in compaction procedures.

The general behaviour of pores in the compacted body can be categorized into three predominant experimental elements:

a. The average pore radius

b. The distribution of the pores around the average radius

c. The existence of large pores evidenced by long "tails" in the pore size distribution curves.

The distribution of the pores around the average radius is due predominantly to the variation in the particle-particle distances, whereas the larger pores can be attributed to the inter-agglomerate voids.

The green compact consolidated without use of lubricant or relaxation resulted in weak green strength and endcapping, due to the highly non-uniform stress transmission throughout the powder. The powder had the lowest compactibility for any available commercial powders due to the high percentage of needlelike morphology. Control of the compaction rate during compaction remained one of the key elements in obtaining the dry compacts without cracking. Thus, compaction rates less than 0.1 cm/min were used for all dry compaction. The pore size distribution obtained for these dry compacts yielded to these physical features: a relatively large average pore size with a broad distribution as well as considerable volume of larger pores.

The potentially important phenomena are the effects of relaxation and of a low viscosity lubricant. Through stress relaxation, heterogeneous density gradients are substantially alleviated, as shown through the more uniform pore size distribution. Thus cracking or endcapping at the punch-powder interface may be prevented with relaxation at a sufficiently slow compaction rate.

The effect of relaxation was also evident when comparing the pore size distribution of binder coated powders, commercially utilized for compaction, with that of relaxed dry compacts. The pore size distribution characteristics of the compacts using binders was between re-

laxed and non-relaxed dry compacts in all three characteristics stated earlier. This again indicates the beneficial effect of relaxation.

Polymer lubrication further aided in the powder rearrangement and relaxation of the inhomogeneous stress transmission through the presence of a viscous flow medium acting as the lubricant. There was a marked decrease of larger pores when using the viscous polymer for both the relaxed and non-relaxed case: the relaxed compact yielding a negligibly small volume of the larger pores. The lubricant possibly acts as an effective means of agglomerate breakdown, especially when stress relaxation is allowed. Similar results were obtained for the same powder used for injection molding process (Ba85). The larger pores present in the injection molded green body and posed problems during sintering disappeared with the use of a viscous polymer utilized in the injection molding process. It is interesting to note that there exists an optimal viscosity of the particulate system. Lower viscosity results in a more uniform stress field within the compact but a less effective load for agglomerate breakdown. Increasing the load resulted in a decrease of the amount of larger pores, while sacrificing the uniform pore size distribution around the mean pore size.

The result of heating the polystyrene lubricant beyond its glass transition temperature (Tg) of 130°C is very pronounced and again emphasize the significance of the viscous flow phenomena as the process control tool for obtaining more uniform green compacts. The heat treatment subsequent to the initial compaction softened the polystyrene and induced further rearrangement through viscous flow under low load.

The best results were obtained for the polymer-lubricated, relaxed and heat treated compact.

An interesting phenomenon found in the pore studies is the effect of load. Earlier studies have reported the decrease in average pore radius with increasing compaction pressure for dry or binder-lubricated powders. The study conducted here also indicates this phenomenon. Furthermore, for dry compacts, the pore size distribution curves demonstrate sharper pore distribution around the average pore radius with increasing load, without alleviating the volume of the larger pores. The fact that the total extent of the larger pores remained almost identical for all three loads for the dry compact indicates that the increased compaction pressure for the dry, relaxed powder compact was not sufficient to break-down the agglomerates and thus, not eliminating the volume of the larger pores between them. Controlling the compact viscosity remains the key element in the die compaction process if uniform green structure is desired.

The interesting and potentially significant physical effect of polymer lubrication, relaxation and compaction parameters such as load and compaction rate of the green compacts were controlled to optimize pore size distribution. The study of the compact uniformity were extended to early stage sintering, confirming the influence of processing on the characteristics of the final product.

APPENDIX A (Lo81)

1. Calculations of Pore Radius

When Hg is forced under pressure into a pore of radius r and length l, the area of volume of mercury external to the pore decreases by

$$A = - 2\pi rl \tag{A1}$$

assuming cylindrical pores. The work required is

$$W_1 = - 2\pi rl \cos\theta \tag{A2}$$

The term $\cos\theta$ is introduced because the force tending to drive the mercury out of the pore act through the contact angle, θ. The work required to force the mercury into the cylindrical pore is given by the applied pressure times the pore length or

$$W_2 = p\pi r^2 l \tag{A3}$$

Since W_1 must equal W_2 equations (2) and (3) can be combined to give

$$Pr = - 2\gamma\cos\theta \tag{A4}$$

In the present study surface tension, γ, is taken as 480 ergs/cm^2 and θ as 140°.

2. Pore Size Distribution

Allow dV to be the volume element of all pores with radii between r and r + dr.

Then,

$$dV = D_v P(r)\, dr \tag{A5}$$

where $D_v(r)$ is the volume pore size distribution function defined as the volume per unit length.

Differentiation of eqn. (A4), assuming constancy of γ and Θ yields

$$Pdr + rdP = 0 \tag{A6}$$

combining eqns. (A5) and (A6) yields

$$-dV = D_v(r)\ r/P\ dP \tag{A7}$$

Then

$$D_v(r) = -(P/r)(dV/dP) \tag{A8}$$

Since change in volume is measured as a decreasing volume, the negative sign can be eliminated to give

$$D_v(r) = (P/r)\ (dV/dP) \tag{A9}$$

APPENDIX B (Hs85c)

The stress-strain relationship for the spring dashpot (Fig. 14) model is

$$\varepsilon = \frac{\sigma}{E_1} + \frac{\sigma}{E_2+\eta\ d/dt} \tag{B1}$$

where E_1 and E_2 are the elastic constants of the springs, η is the viscosity of the dashpot, and σ and ε are the stress and strain, respectively. This model is used to describe the viscous polymer particulate system used in the present analysis. Rearrangement of eqn. (B1) gives,

$$\eta\dot{\sigma} + (E_1 + E_2)\ \sigma = E_1(\eta\dot{\varepsilon} + E_2 t) \tag{B2}$$

Using eqn. (B2), an experiment can be designed to determine the parameters E_1, E_2 and η. In the experiment, the material is initially subjected to a constant strain rate, $\dot{\varepsilon}_0$, during the time interval $0 \leq t \leq t_f$, and the stress reaches σ_f at $t = t_f$. The total strain $\varepsilon = \dot{\varepsilon}_0 t_f$ is then held ($\dot{\varepsilon} = 0$) for $t \geq t_f$, and the stress is relaxed viscoelastically. The stress solutions for the loading ($\dot{\varepsilon} = \dot{\varepsilon}_0$) and the holding ($\varepsilon = 0$) conditions can be derived from eqn. (B2) such that,

$$\sigma_t = \frac{E_1^2}{(E_1+E_2)^2}\,\eta\dot{\varepsilon}_0 \left\{1 - \exp\left(-\frac{E_1+E_2}{\eta}\,t\right)\right\} + \frac{E_1E_2}{E_1+E_2}\,\dot{\varepsilon}_0 t \qquad (0\leq t\leq t_f) \tag{B3a}$$

$$\sigma(t) = \sigma_f \exp\left[-\frac{E_1+E_2}{\eta}\,(t-t_f)\right] + \frac{E_1E_2}{E_1+E_2}\,\dot{\varepsilon}_0 t_f \left\{1-\exp\left[-\frac{E_1+E_2}{\eta}\,(t-t_f)\right]\right\} \qquad (t\geq t_f) \tag{B3b}$$

The viscosity, η, can then be determined from experimental stress-time curve.

Differentiation of eqn. (B3a) at t = 0 yields,

$$E_1 = \dot{\sigma}(0)/\dot{\varepsilon}_0 \tag{B4}$$

As $t = \infty$, eqn. (B3b) can be reduced to

$$\sigma_\infty = \frac{E_1 E_2}{E_1+E_2}\,\dot{\varepsilon}_0 t_f \tag{B5}$$

where σ is the steady state stress during the holding. To measure the viscosity, a time parameter, t^* is introduced, which is defined by,

$$t-t_f = \frac{\eta}{E_1+E_2} = t^* \tag{B6}$$

Combining eqns. (B3b), (B5) and (B6) yields,

$$\sigma = \sigma_\infty + (\sigma_f-\sigma_\infty)e^{-1} \qquad (t=t_f+t^*) \tag{B7}$$

where e is the Napierian number. The time parameter, t^*, can then be determined from eqn. (B7) and Fig. 1. Furthermore, at $t = t^*$ eqn. (B3a) can be reduced to

$$E_2 = \frac{E_1}{\left(1 - \dfrac{\sigma^*}{E_1\dot{\varepsilon}_0 t^*}\right)e} - E_1 \tag{B8}$$

Substitution of eqn. (B8) into eqn. (B6) yields

$$\eta = \frac{E_1 t^*}{\left(1 - \dfrac{\sigma^*}{E_1\dot{\varepsilon}_0 t^*}\right)e} \tag{B9}$$

APPENDIX C

Under constant strain rate, $\dot{\varepsilon}$, the stress and the strain rate relation for a material satisfying a Maxwell model, can be described as

$$\sigma = \eta\dot{\varepsilon}(1-e^{-G/\eta t}) \tag{C1}$$

where η and G are the viscosity and shear modulus, respectively, of the material. Furthermore, the linear strain rate, $\dot{\varepsilon}$, and the densification rate, $\dot{\rho}$, can be related by (Hs85)

$$\dot{\varepsilon} = -\frac{\dot{\rho}}{3\rho} \tag{C2}$$

Integration of eqn. (C2) yields

$$\dot{\varepsilon}t = -1/3 \ln \frac{\rho}{\rho_0} \tag{C3}$$

where ρ_0 is the initial density at t = 0. Combination of eqns. (C1) and (C3) gives

$$\frac{\sigma}{\eta\dot{\varepsilon}} = 1 - \left(\frac{\rho}{\rho_0}\right) G/3\eta\dot{\varepsilon} \tag{C4}$$

REFERENCES

Ba85 G. Bandyopadhyay, "Injection Molding of Silicon Nitride: Recent Developments," presented at the 87th Annual Meeting, ACS, May 5-9, 1985.

Br81 J. A. Brewer, R. H. Moore, and J. Reed, "Effect of Relative Humidity on the Compaction of Barium Titanate and Manganese Zinc Ferrite Agglomerate containing Polyvinyl Alcohol," Am. Ceram. Bull. 60 (2) 212-20 (1981).

Bo78a D. W. Bowen and R. W. Taylor, "Silica Viscosity from 2300 - 2600K", Am. Ceram. Bull. 57 (9) 818-19 (1978).

Bo78b L. J. Bowen, R. J. Weston, T. G. Carruthers, and R. J. Brook "Hot Pressing and the Alpha to Beta Transformation in Silicon Nitride", J. Mater. Sci. 13 (2) 341-50 (1978).

Bo78c L. J. Bowen and T. G. Carruthers, "Dev. of Mechanical Strength in Hot Pressed Si_3N_4" J. Mater. Sci Lett. 13 (3) 684-89 (1978).

Bo66 G. Bockstiegel, "Relation Between Pore Structure and Densification Mechanism in the Compacting of Iron Powder," Int'l. J. of Powder Metall. 2 (4) 13-26 (1966).

Br83 A. Broese Van Gronenou and R. C. D. Lissenburg, "Inhomogeneous Density in Die Compact: Experiment and Finite Element Calculation," J. Am. Ceram. Soc., 66 (9) C156-7 (1983).

Br82 R. J. Brook, "Fabrication Principle for the Production of Ceramics with Superior Mechanical Properties," Eng. Ceram. Proceeding of the First, British Ceram. Soc. Stokes on Trent 32 (3) 7-23 (1982).

Br81 A. Broese Van Aronenou, "Compaction of Ceramic Powders," Powder Technol. 28 221-8 (1981).

Ca84 M. M. Carroll and K. T. Kim, "Pressure Density Equation for Porous Metals and Metal Powders," Powder Metall. 2F (3153) 153-9 (1984).

Ca82 S. S. Campbell and S. Dutta, "Effects of Healing Rate on Density, Microstructure and Strength of Si_3N_4-6 wt% Y_2O_3 and a SIALON," J. Am. Ceram. Soc., 61 (8) 854-6 (1982).

Cl82 D. R. Clarke, "Densification of Si_3N_4 - Effect of Impurity," J. Am. Ceram. Soc., 65 (2) c21-3 (1982).

Cl84 D. R. Clarke, "The Microstructure of Nitrogen Ceramics," Progress in Nitrogen Ceramics, F. Riley eds., Nijhoff Pubs., 341-58 (1984).

Cl81 D. R. Clarke, N. J. Zaluzlc, and R. W. Carpenter, "Intergranular Phase in Hot Pressed Si_3N_4 I: Elemental Composition," J. Am. Ceram. Soc. 64 (10) 601-7 (1981).

Cl77 D. R. Clarke et. al., "Grain Boundary Phase in Hot Pressed Si_3N_4," J. Am. Ceram. Soc., 60 (11-12) 491 (1977).

Co62 A. R. Cooper and L. E. Eaton, "Compaction Behavior of Several Ceramic Powders," J. Am. Ceram. Soc., 45 (3) 97-101 (1962).

Cr78 T. D. Croft et. al., "Microstratified Mixing of Ceramic System's Viscosity Dependence," Am. Ceram. Soc. Bull. 57 (12) 1111-5 (1978).

Cu78 I. B. Cutler, "Active Powder," from p. 217 Ceramic Process Before Firing, G. Onoda eds., John Willy and Sons Pubs. (1978).

Di84 R. A. Dimilva and J. Reed, "Stress Transmission During the Compaction of a Spray Dried Alumina Powder in a Steel Die," J. Am. Ceram. Soc., 66 (9) 667-72 (1984).

Di83 R. A. Dimilva and J. S. Reed, "Dependence of Compaction on the Glass Transition Temperature of the Binder Phase," Am. Ceram. Bull. 62 (4) 84-8 (1983).

Dr81 R. A. L. Drew, S. Hampshire, and K. H. Jack, "Nitrogen Glasses Specimens," Sp. Ceram. 7, B.C.R.A., 6 (33) D. Taylor and P. Popper eds., Stokes on Trent (1981).

Du82 S. Dutta, "Microstructures and Drop Characteristic of Sintered Si_3N_4, SiC and SIALON," J. Am. Ceram. Soc., 65 (1) c2-3 (1982).

Dy84 F. W. Dynys and J. W. Holloran, "Influence of Aggregates on Sintering," J. Am. Ceram. Soc., 67 (9) 596-601 (1984).

Dy83 F. W. Dynys and J. W. Holloran, "Compaction of Aggregate Alumina Powders," J. Am. Ceram. Soc., 66 (4) 655-9 (1983).

Ev71 A. G. Evans and J. V. Sharp, "Microstructure Studies on Silicon Nitride," J. Mater. Sci., 6 (10) 1292-301 (1971).

Fa68 R. J. Fariss, "Prediction of Viscosity of Multimodal Suspensions from Unimodal Viscosity Data," Trans. Soc. Rheology, 12 (1) 281 (1968).

Fe72 T. J. Fennelley and J. Reed, "Mechanics of Pressure Slip Casting," J. Am. Cream. Soc., 55 (5) 264-8 (1972).

Fi83 H. F. Fischmeister and E. Alzc, "Densification of Powders by Particle Deformation," J. Powder Metall., 26 (2) 82-9 (1983).

Fr84 K. W. French, C. L. Quackenbush, J. S. Smith, and J. T. Neil, " Sintering Property and Fabrication of Si_3N_4/Y_2O_3 based Ceramics," Progress in Nitrogen Ceramics, F. Riley eds., Nijhoff Pubs., (1984).

Fr84 R. G. Frey and J. W. Holloran, "Compaction Behavior of Spray Dried Alumina," J. Am. Ceram. Soc., 67 (3) 199-203 (1984).

Ga74 G. E. Gazza "Hot Pressed Si_3N_4," J. Am. Ceram. Soc., 56 (12) 662-63 (1974).

Ga79 F. Galasso and R. Veltri, "Sintering of Si_3N_4/Y_2O_3 under high N_2 Pressure," J. Am. Ceram. Bull., 58 (8) 793-94 (1979).

Gr77 C. Greskovich, S. Prochazka and J. H. Rosolowski, "The Sintering Behavior of Covalently-Bonded Materials," Nitrogen Ceramics, F. Riley eds., Noordhoff Pubs., (1977).

Gr78 C. Greskovich and C. Oclair "Effect of Impurity on Sintering of Si_3N_4 Containing MgO or Y_2O_3 Additions," Am. Ceram. Soc., 57 (11) 1055-56 (1979).

Gr80 C. Greskovich and J. A. Palm, "Controlling the O_2 Contents of Si_3N_4 Powders," Am. Ceram. Soc. Bull., 59 (11) 1155-56 (1980).

Gr81a C. Greskovich, "Preparation of High density Si_3N_4 by a Gas Pressure Sintering Process," J. Am. Ceram. Soc., 64 (12) 725-30 (1981).

Gr81b C. Greskovich and S. Prochazka, "Stability of Si_3N_4 and Liquid Phase during Sintering," J. Am. Ceram. Soc. 64 (7) C96-7 (1981).

Gr84 C. Greskovich " A Gas Pressure Sintering Process for Producing Dense Silicon Nitride," Progress In Nitrogen Ceramics, F. Riley eds., Nijhoff Pubs., (1984).

Gu72 T. K. Gupta, "Possible Correlation between density and grain size during Sintering," J. Am. Ceram. Soc., 55 (5) 276-77 (1972).

Gu84 I. Ya Guzman, A. V. Dovbysg, N. M. Denisova and E. V. Soloduk-hina, "Casting Silicon Nitride Products from Silicon Slip" 645-47 (1984).

Ha81 S. Hampshire and K. H. Jack, "The Kinetics of Densification and Phase Transformation of N_2 Ceramics," Sp. Ceram. 7 Brit. Ceram. Research Assn. 31 (6) 37-49 (1981).

Ha84 S. Hampshire and K. H. Jack, "Densification and Transformation Mechanisms in N_2 Ceramics," Progress in N_2 Ceramics, F. Riley eds., Nijhoff Pubs. (1984).

He61 R. W. Heckel "Density Pressure Relationships in Powder Compaction," Trans. Met. Soc., AIME, 221 671-75 (1961).

He84 J. Heinrich, "Contribution of the Strength-Porosity Relationship in Reaction Bonded Silicon Nitride," Progress in N_2 Ceramics, F. Riley eds., Nijhoff Pubs. (1984).

He84 L. Hench and D. Ulrich eds., Ultrasonic Processing of Ceramics, Glasses and Composites, Wiley and Sons (1984).

Hs82 C. H. Hsueh, A. G. Evans, R. L Coble, "Microstructural Development during Final and Intermediate Stage Sintering I - Pore Grain Boundary Separation," Acta. Metall., 30 1269-79 (1982).

Hs85a C. H. Hsueh, A. G. Evans and L. C. DeJonghe, "Sintering of Glass" to be published.

Hs85b C. H. Hsueh, A. G. Evans, R. M. Cannon and R. J. Brook, "Viscoelastic Stresses and Sintering Damage In Heterogeneous Powder Compacts," Acta. Metall., in press.

Hs85c C. H. Hsueh, "A Mathematical Model of Viscosity Measurement for Viscoelastic Solids" to be published.

Ik84 T. Ikegami and Y. Moriyoshi, "Intermediate Stage Sintering of Homogeneously Packed Compact," J. Am. Ceram. Soc., 67 (3) 174-78 (1984).

Is83 G. Isik and P. F. Messer, "The Effect of Compaction Pressure on Coarsening of Open Pores in Fired Compacts from Agglomerated Powder," Fab. Sci. 3, Brit. Ceram. Research Ass., 5 (66) 39-50 (1983).

Ja72 P. J. James, "Fundamental Aspects of Consolidation of Powders," Powder Metall. Int'l. 4(2) 82; (3) 145; (4) 193; (1972).

Ja84 K. H. Jack, "The Characteristics of SIALONS and the Relationships in SIALON and Silicon Nitrides," Progress in N_2 Ceramics, F. G. Riley ed., Nijhoff Pubs., Boston, Mass.(1984).

Jo81 D. W. Johnson Jr., "Nonconventional Powder Preparation Technique", J. Am. Ceram. Bull., (60) 2 221-24 (1981).

Ka84a R. N. Katz, "Nitrogen Ceramics 1976-1981", Progress in N_2 Ceramics, E. G. Riley ed., Nijhoff Pubs., Boston, Mass. (1984).

Ka84b R. Katz and R. B. Schultz, "U. S. National Programs in Ceramic for Energy Conversion", Progress in N_2 Ceramics, E. Riley ed., Nijhoff Pubs., Boston, Mass. (1984).

Ki59 W. D. Kingery, "Liquid Phase Sintering," J. Appl. Phys. 30 301 (1959).

Kn84 H. Knoch, K. A. Schroetz and A. Lipp, "Microstructural Development in Silicon Nitride," Progress in N_2 Ceramics, F. Riley ed., Nijhoff Pubs., Boston, Mass. (1984).

Ko83 K. Komeya, "Development of N_2 Ceramics", Toshiba Internal Report.

Kr79 O. L. Krivanek, T. M. Shaw and G. Thomas, "The Microstructure and Distribution of Impurity in Hot Pressed and Sintered Silicon Nitride," J. Am. Ceram. Soc., 62 (11) 585-90 (1979).

La81a F. F. Lammers, C. Styuck, F. A. Varkeussa, J. Dolderman and C. J. deBlary "Evaluation of Force-displacement during one sided die compaction," Powder Technol., 28 147-165 (1981).

La81b A. Lawrey, "Powder Consolidation," Ceramic Processing Before Firing, L. Hench & G. Onoda eds., John Wiley and Sons (1978).

La82 M. H. Lewis and R. J. Lumby, "Nitrogen Ceramics: Liquid Phase Sintering," Powder Metall., 26 (2) 73-81 (1983).

La84a F. F. Lange "Sinterability of Agglomerate Powder", J. Am. Ceram. Soc., 67 (2) 83-9 (1984).

La84b H. T. Larker, "HIPing of Ceramics," Progress in N_2 Ceramics, F. Riley eds., Nijhoff Pubs., Boston, Mass. (1984).

La84c D. C. Larson and J. W. Adams, "The Nature of SiC for Use in Heat Engines as Compared to Si_3N_4: An Overview of Property Difference," Progress in N_2 Ceramics, F. Riley eds., Nijhoff Pubs., Boston, Mass. (1984).

La84d F. F. Lange, "Fabrication and Properties of Dense Polyphase Silicon Nitride," Am. Ceram. Soc. Bull. 1369-1374 (1984).

Le70 D. B. Leser and O. J. Whittemore Jr., "Compaction Behavior of Ceramic Particles," J. Am Ceram. Soc., 49 (8) 714 (1970).

Le83 M. H. Lewis and R. J. Lumby, "Nitrogen Ceramics: Liquid Phase Sintering," Powder Metall. 28 (2) 73-81 (1983).

Lo80 R. E. Loehman and D. J. Rowcliffe, "Sintering of Si_3N_4-Y_2O_3-Al_2O_3," J. Am. Ceram. Soc., 63 (3-4) 144-48 (1980).

Lo81 S. Lowell and J. E. Shields, "Pore Spectra from Cont. Scan Hg Porosimetry," Powder Technol. 28 (1981) 201-4.

Lu78 S. J. Lukasiewicz and J. Reed, "Character of Compaction Response of Spray Dried Agglomerate," J. Am. Ceram. Bull. 57 (9) 798-801 (1978).

Ma83 J. A. Mangels and R. M. Williams, "Injection Molding of Ceramics to High Green Densities," J. Am. Ceram. Bull. 62 (5) 601-10 (1983).

Me78 D. R. Messier, F. L. Riley and R. J. Brook, "The α/β Silicon Nitride Phase Transformation," J. Mater. Sci. 13 (6) 1199-1205 (1978).

Me82 G. Y. Messing, C. J. Markhoff and L. G. McCoy, "Character of Ceramic Powder Compact," J. Am. Ceram. Soc., 61 (8) 857-60 (1982).

Mo76 D. R. Mosher et. al., "Measurement of Viscosity of the Grain Boundary Phase in Hot Pressed Si_3N_4'" J. Mater. Sci. 11 49-53 (1976).

Mo81 L. Moscon and S. Lub, "Practical Use of Hg Porosimetry in Study of Porous Solids," Powder Technol., 29 45-52 (1981).

Mo84a M. Mori, H. Inoue and T. Ochiai, "Preparation of Silicon Nitride Powder From Silica," Nitrogen Ceramics, F. Riley eds., Noordhoff Pubs., 149-55 (1981).

Mo83 B. C. Motsuddy, "Influence of Powder Characteristics on the Rheology of Ceramic in Molding Mixture," Fab. Sci.3, Brit. Ceram. Research. Assoc., 33 (5) 117-37 (1983).

Mo84b I. H. Moon and K. H. Kim, "Relation Between Compacting Pressure Green Density and Green Strength of Cu Powder Compacts," Powder Metall., 27 (2) 80-4 (1984).

Ni78 D. E. Nies and R. B. Bennett, "Structure and Properties of Agglomerates," Ceramic Processing before Firing, L. Hench & G. Onoda eds., Wiley and Sons Pubs., (1978).

Ni84a C. W. Nies and G. L. Messing, "Binder Hardness and Plasticity in Granule Compaction" 58-66 (1984).

Ni84b C. W. Neiss and G. L. Messing "Effect of glass Transition Temperature of Polyethylene Glycol-Plasticized Polyvinyl Alcohol on granule Compaction," J. Am. Ceram. Soc., 67 (4) 301-4 (1984).

Od78 I. Oda, M. Kaneno and Y. Yamamoto, "Pressureless Sintered Silicon Nitride," Nitrogen Ceramics, F. Riley eds., Nijhoff Pubs., Boston, Mass.(1977).

On85 G. Y. Onoda, "Overview of Additives Organics for Ceramic Processing," presented at 87th Annual Meeting of the Am. Ceram. Soc., Cinn., Ohio (1985).

On81 G. Y. Onoda and M. A. Jannery, "Application of Soil Mechanics Concepts to Ceramic Particulate Processing," from Advances in Powder Technology, G. Y. Chin eds., American Soc. of Metals, Park, Ohio, (1981).

Or78 C. Orr Jr, " Physical Characterization Technique for Powders," Ceramic Processing Before Firing, L. Hench and G. Onoda eds., Wiley and Sons, 39-59 (1978).

Pa84a Paramanand and P. Ramakrishnan, "Effect of Powder Characterization on Compaction Parameter and Ejection Pressure of Compacts," Powder Metall., 27 (3) 163-68 (1984).

Pa84b A. E. Pasto, "Causes and Effects of Fe-bearing Inclusions in Sintered Si_3N_4," J. Am. Ceram. Soc., 67 (9) c178-180 (1984).

Pa83 V. V. Pankov, M. Paulus and A. Dubson, "Powder Preparation for Rapid Sintering by Combination Suspension Solution Freeze Drying Technique," Fab. Sci. 33 (3), British Ceramic Research Ass., Stokes on Trent 17-31 (1983).

Po84 P. Popper, "Sintering of Silicon Nitride, A Review", Progress in Nitrogen Ceramics, F. Riley eds., Nijhoff Pubs., Boston, Mass. (1984).

Po81 R Pompe, L. Eklund and L. Hermasson, "Investigation of the Role of the Protective Powders in the Sintering of Si_3N_4 Based Powders," Special Ceramics 7, Brit. Ceram. Research Ass. 31 (6) 97-105 (1981).

Po61 P. Popper and S. N. Ruddelson, "The Preparation, Property and Structure of Si_3N_4," Trans. Brit. Ceram. Soc., 9 (6) 603-26 (1961).

Pr78 S. Prochazka and C. Greskovich, "Synthesis and Characteristic of Pure Si_3N_4 Powder," J. Amer. Ceram. Soc. 57 (6) 579-86 (1978).

Ra82 E. M. Rabinovich et. al., "Slip Casting of Si_3N_4 for Pressureless Sintering," J. Mater. Sci 17 323-28 (1982).

Ri80 F. L. Riley, "Silicon Nitride: An Overview," Science of Ceramics 12 - Ceramurgica S. R. L., Fraenza, 15-25 (1980).

Ri73 D. W. Richerson, "Effect of Impurities on the High Temperature Properties of Hot Pressed Si_3N_4," Am. Ceram. Soc. Bull., 52 (7) 560-89 (1973).

Ro84 G. C. Robinson, "The Relationship between Pore Structure of Brick," Am. Ceram. Soc. Bull., 63 (2) 295-300 (1984).

Ro81 W. H. Rhodes, "Agglomerate and Particle Size Effects on Sintering of Yittria Stabilized Zirconia," J. Am. Ceram. Soc., 64 (1) 19-22 (1981).

Ro71 H. M. Rootare and A. C. Nyce, "The Use of Porosimetry in the Measurement in Pore Size Distribution in Porous Materials," Int'l J. Pow. Metall. 7 (1) 3-11 (1971).

Ro70 R. C. Rossi et. al., "Quantitative Analysis of the Mixing of Fine Powders," J. Am. Ceram. Bull., 49 (3) 289-313 (1970).

Sa84 Y. Sano and K. Miyagi, "Dynamic Compaction and the Effect of Air Contained within the Powder Pores," Int'l J. of Powder Metall. & Pow. Technol., 20 (4) 115-129 (1984).

Sc84 G. Schwier, "On the Preparation of Fine Silicon Nitride Powders," Progress in Nitrogen Ceramics, F. Riley eds., Nijhoff Pubs., Boston Mass, (1984).

Sc65 E. G. Schwartz and A. S. Weinstein, "Model for Compaction of Ceramic Powders," J. Am. Ceram. Soc., 48 (7) 346-50 (1965).

Sc49 K. Schwaetzwalder, "Inj. Molding of Ceramic Materials," Am. Ceram. Soc. Bull., 28 (11) 459-62 (1949).

Si82 A. R. E. Singer, "The Challenge of Spray Forming," Pow. Metall., 25 (4) 195-200 (1982).

So84 S. Somiya et. al., "Hot Isostatic Pressing of Shocked Si_3N_4 Powder," J. Am. Ceram. Soc., 65 (3) C51-52 (1984).

St79 S. Strijbos, A. Broese van Gronenou and P. A. Vermeer, "Recent Progress in Understanding Die Compaction of Powders," J. Am. Ceram. Soc., 62 (1-2) 51-9 (1979).

St76 S. Strijbos, "Friction between Powder Compact and Metal Wall," Science of Ceramics 8, British Ceram. Research Assn., P. Popper eds., Stokes on Trent, 415-27 (1976).

St77 S. Strijbos et. al., "Stresses Occurring during One Sided Compaction of Powders," Pow. Technol. 18 (2) 187-200 (1977).

St77 S. Strijbos, "Powder Wall Friction: The Effects of Orientation of Wall Grooves and Wall Lubricants" Pow. Technol. 18 209-14 (1977).

Sz81 A. Szweda, A. Hendry and K. H. Jack, "The Prep. of Si_3N_4 from Silica by Sol-Gel," Sp. Ceram 7, Brit. Ceram. Research Ass., Stokes on Trent, 107-117 (1982).

Te74 G. R. Terwilliger and F. F. Lange, "Hot Pressing Behavior of Si_3N_4," J. Am. Ceram. Soc., 57 (1) 25-9 (1974).

Ti51 S. P. Timoshenko and J. N. Goodier, "Theory of Elasticity," McGraw-Hill, New York (1951).

Th81a R. Thompson, "Mechanics of Powder Pressing I: Model for Powder Densification," J. Am. Ceram. Soc. 60 (2) 237-43 (1981).

Th81b R. Thompson, "Mechanics of Powder Pressing II: Finite Element Analysis of Endcapping in Pressed Green Compacts," J. Am. Ceram. Soc., 60 (2) 244-47 (1981).

Th81c R. Thompson, "Mechanics of Powder Pressing III: Model for Green Strength of Pressed Powder," J. Am. Ceram. Soc., 60 (2) 248-51 (1981).

Wi83 R. M. Williams and A. Ezis, "Slip Casting of Si Shapes and Their Nitriding," Am. Ceram. Soc. Bull. 62 (5) 607-10 (1983).

Wi81 R. R. Wills and M. C. Brockway, "Hot Isostatic Pressing of Ceramics," Sp. Ceram, 7, Brit. Ceram. Research Ass., Stokes on Trent, 233-247 (1981).

Wh81 O. J. Whittemore, "Hg Porosimetry of Ceramics," Pow. Technol., 29 (1981) 167-75.

Wi83 S. M. Wiederhon and N. J. Tighe, "Structural Reliability of Yittria Doped Hot Pressed Silicon Nitride at Elevated Temperature," J. Am. Ceram. Soc., 66 (12) 884-89 (1983).

Wi83b R. R. Wills et. al., "Silozanes, Silanes and Siliazides in the Preparation of Ceramics and Glasses," J. Am. Ceram. Bull., 62 (8) 904-11 (1983).

Wo84 G. Wohing and R. Carlsson, "Sintering of Silicon Nitride Based Materials Using the Powder Bed Technique," Progress in Nitrogen Ceramics, F. Riley eds., Nijhoff Pubs., Boston, Mass. (1984).

Ye79 H. C. Yeh and P. F. Sikora, "Consolidation of Si_3N_4 by HIP," J. Am. Ceram. Bull., 58 (4) 444-47 (1979).

Yo70 W. S. Young and I. B. Cutler, "Initial Sintering with Constant Rate of Heating," J. Am. Ceram. Soc., 53 (12) 559-63 (1970).

FIGURE CAPTIONS

Fig. 1. Flows chart depicting the experimental procedure.

Fig. 2. A schematic showing stress as a function of time for powder compaction a) without relaxation and b) with relaxation.

Fig. 3. Plot of D_r (volume pore size distribution) versus pore radius for polymer lubricated and dry compacts pressed without relaxation.

Fig. 4. Plot of D_r (volume pore size distribution) versus pore radius for compaction rates of 0.1cm/min and 0.5 cm/min pressed without relaxation. The compacts were polymer lubricated.

Fig. 5. Plot of D_r (volume pore size distribution) versus pore radius for polymer lubricated compacts pressed with relaxation and without relaxation.

Fig. 6. Plot of D_r (volume pore size distribution) versus pore radius for dry compacts pressed with relaxation and without relaxation.

Fig. 7. Plot of D_r (volume pore size distribution) versus pore radius for dry compacts with three values of increasing load. The compacts were relaxed.

Fig. 8. Plot of D_r (volume pore size distribution) versus pore radius comparing compaction of powder with a binder to dry compacts pressed with and without relaxation.

Fig. 9. Plot of D_r (volume pore size distribution) versus pore radius for polymer lubricated and dry compacts pressed with relaxation.

EXPERIMENTAL FLOWCHART

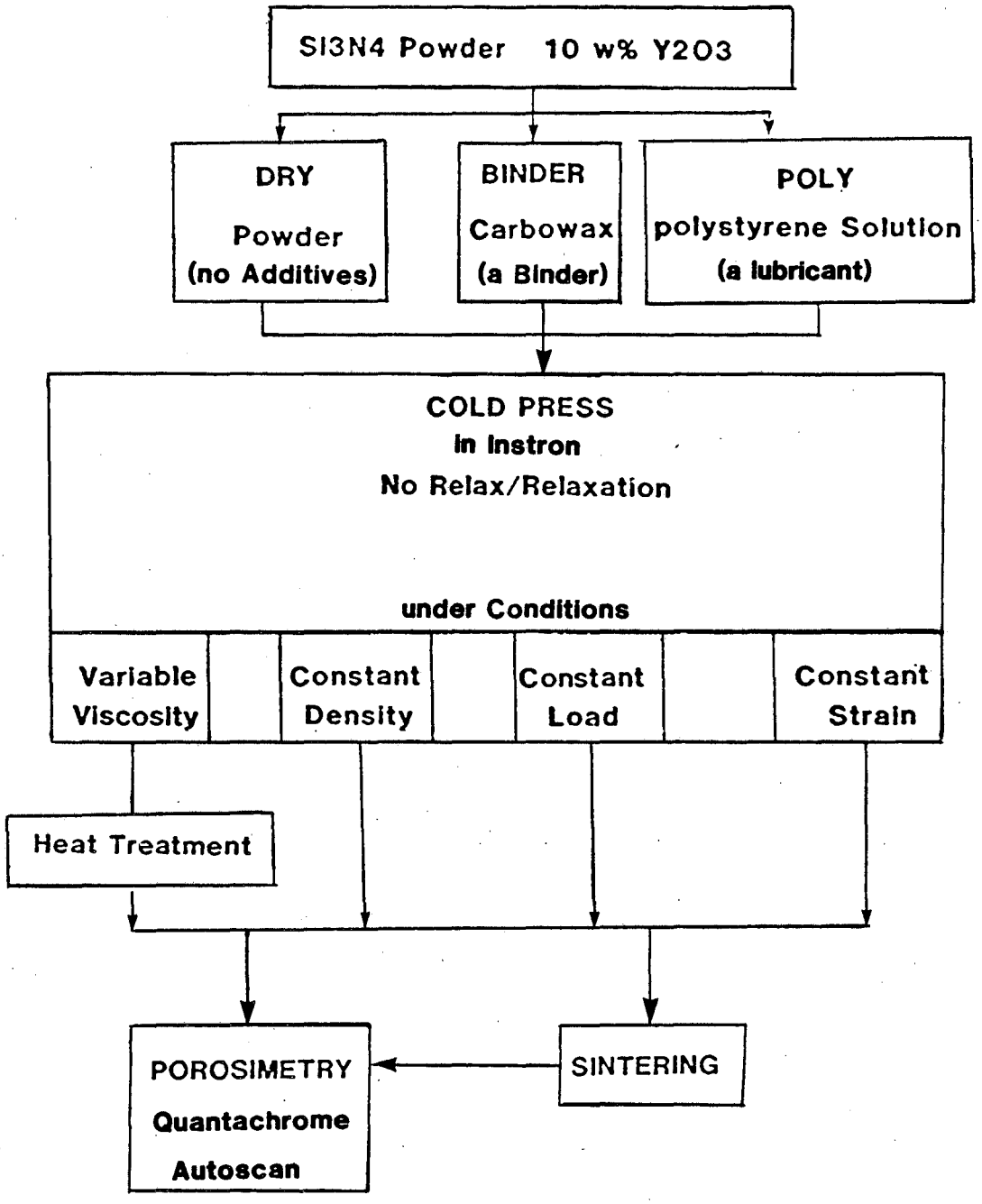

XBL 858-3665

Fig. 1

A. Without Relaxation

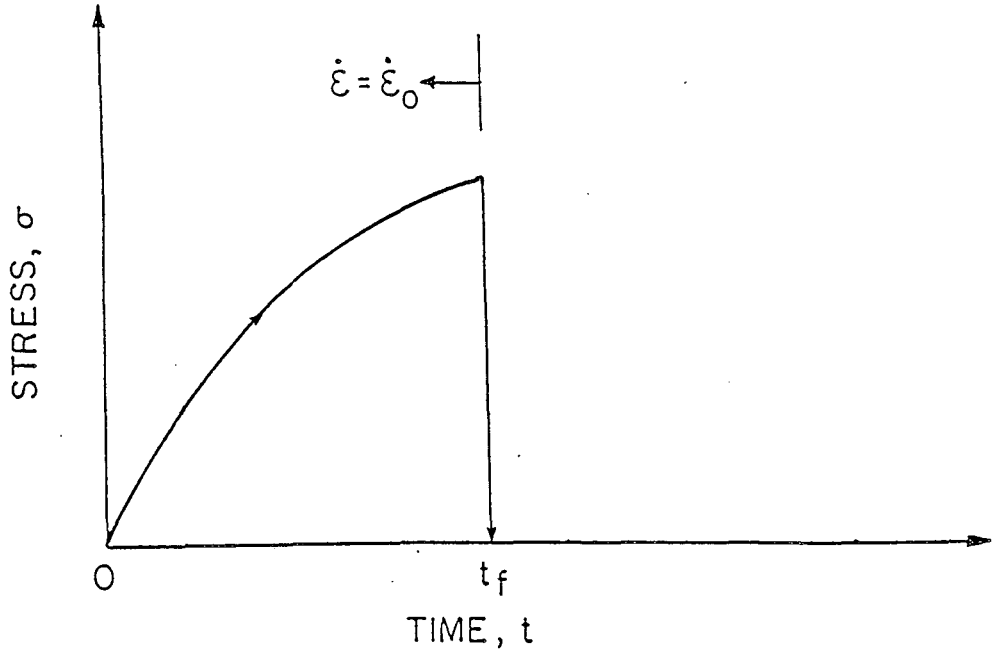

B. With Relaxation

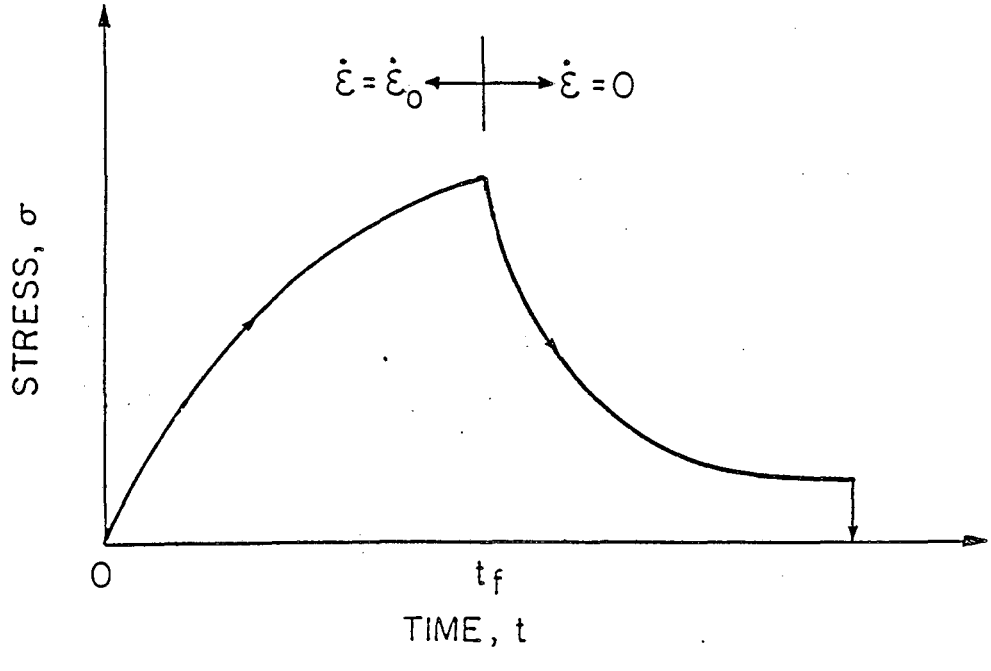

XBL 857-3102

Fig. 2

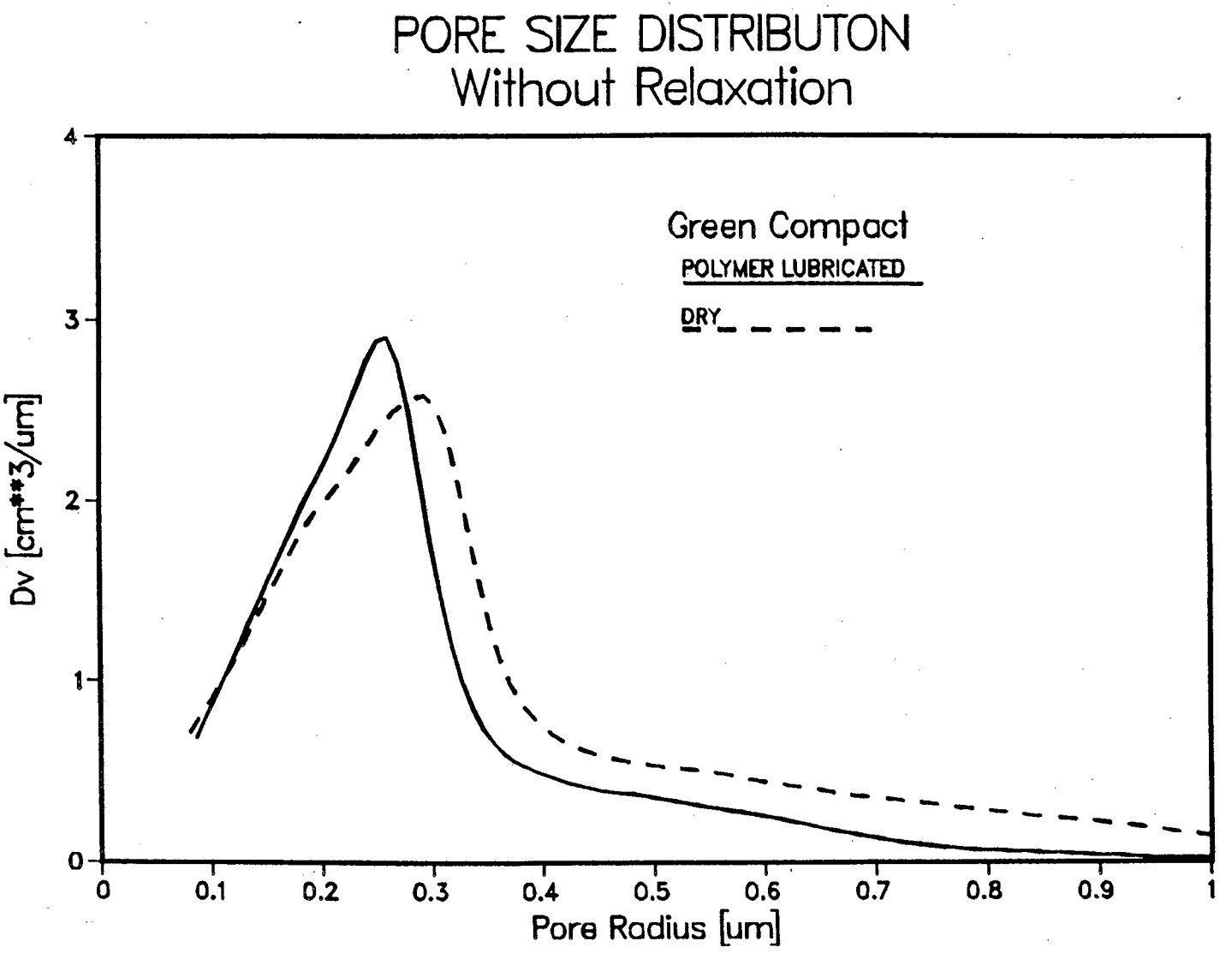

Fig. 3

XBL 857-3099

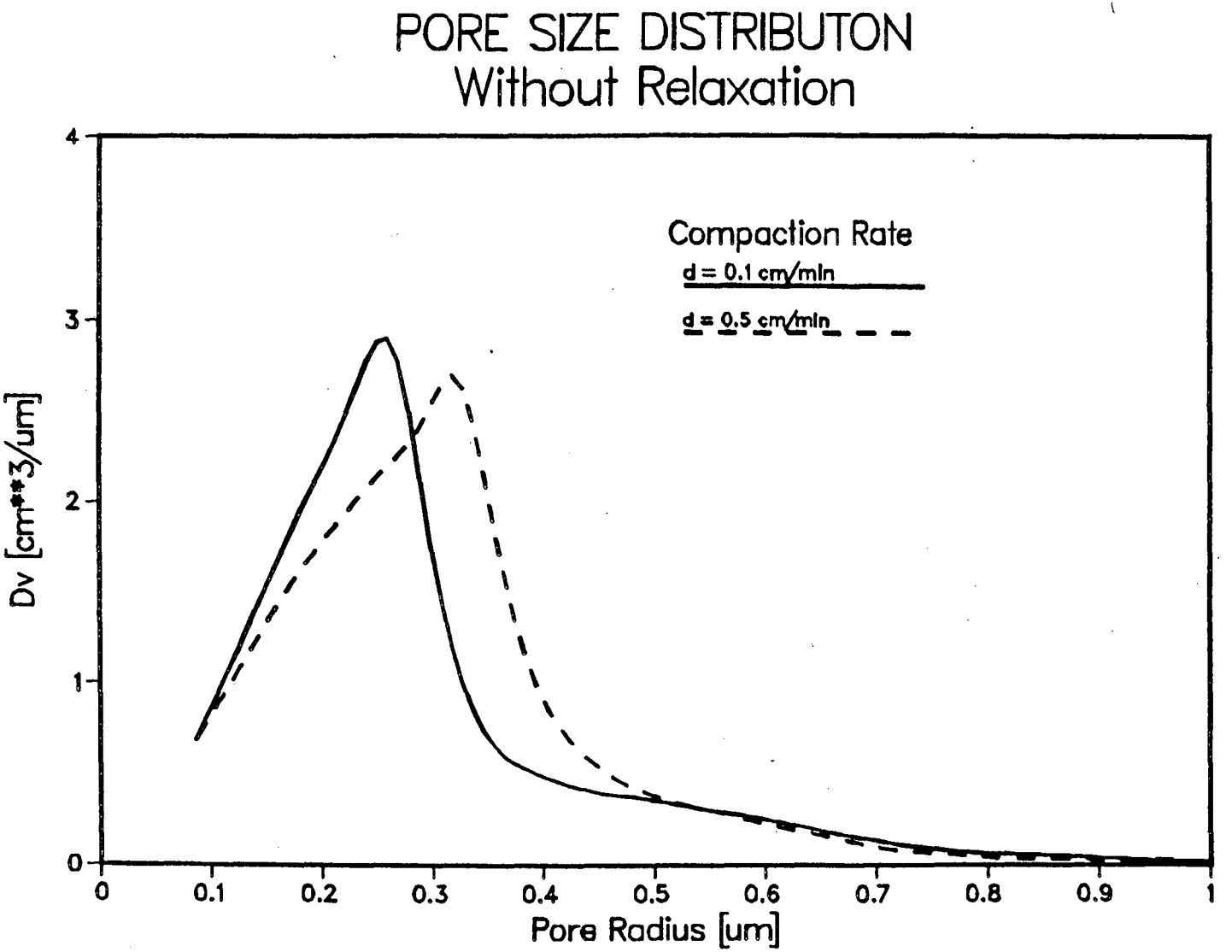

Fig. 4

XBL 857-3100

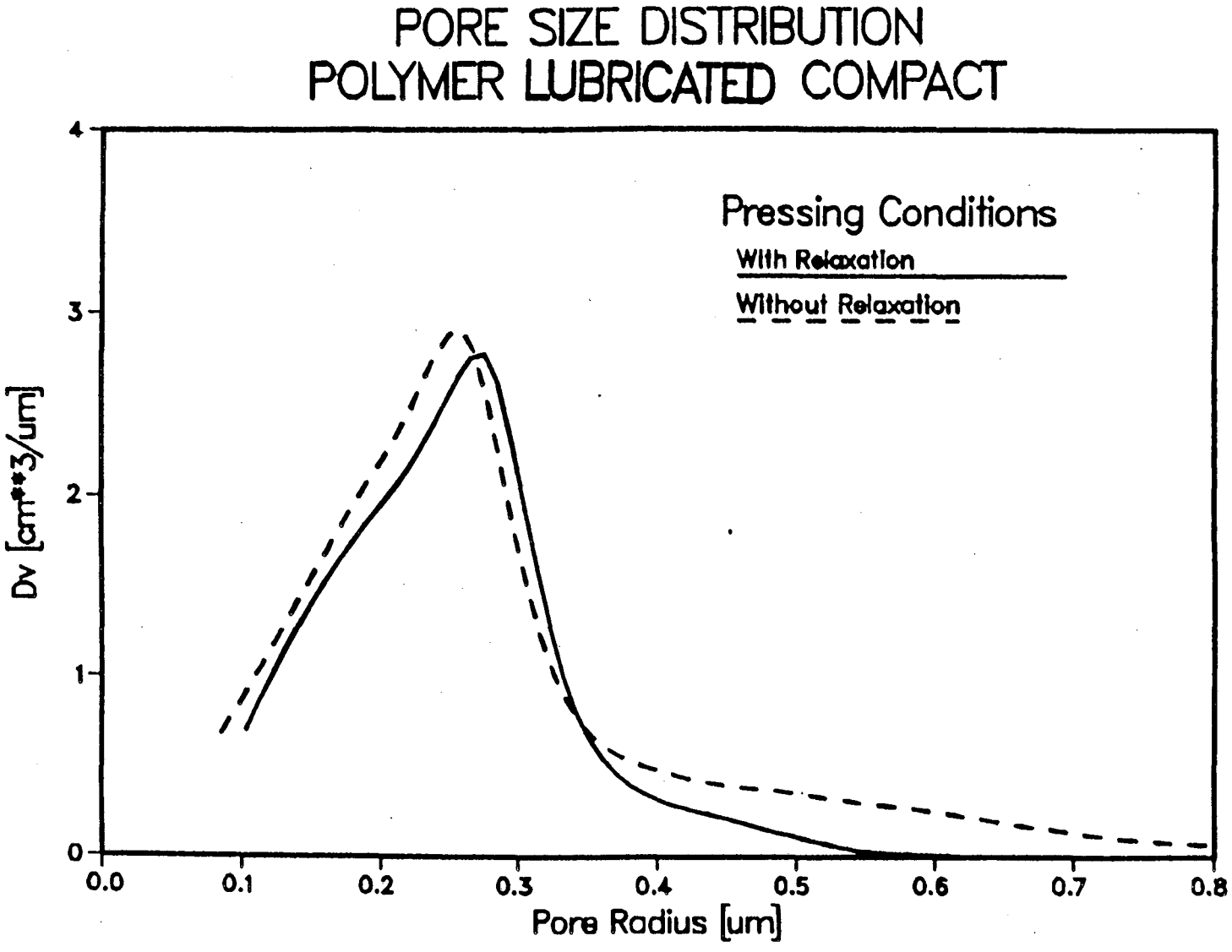

Fig. 5

XBL 857-3097

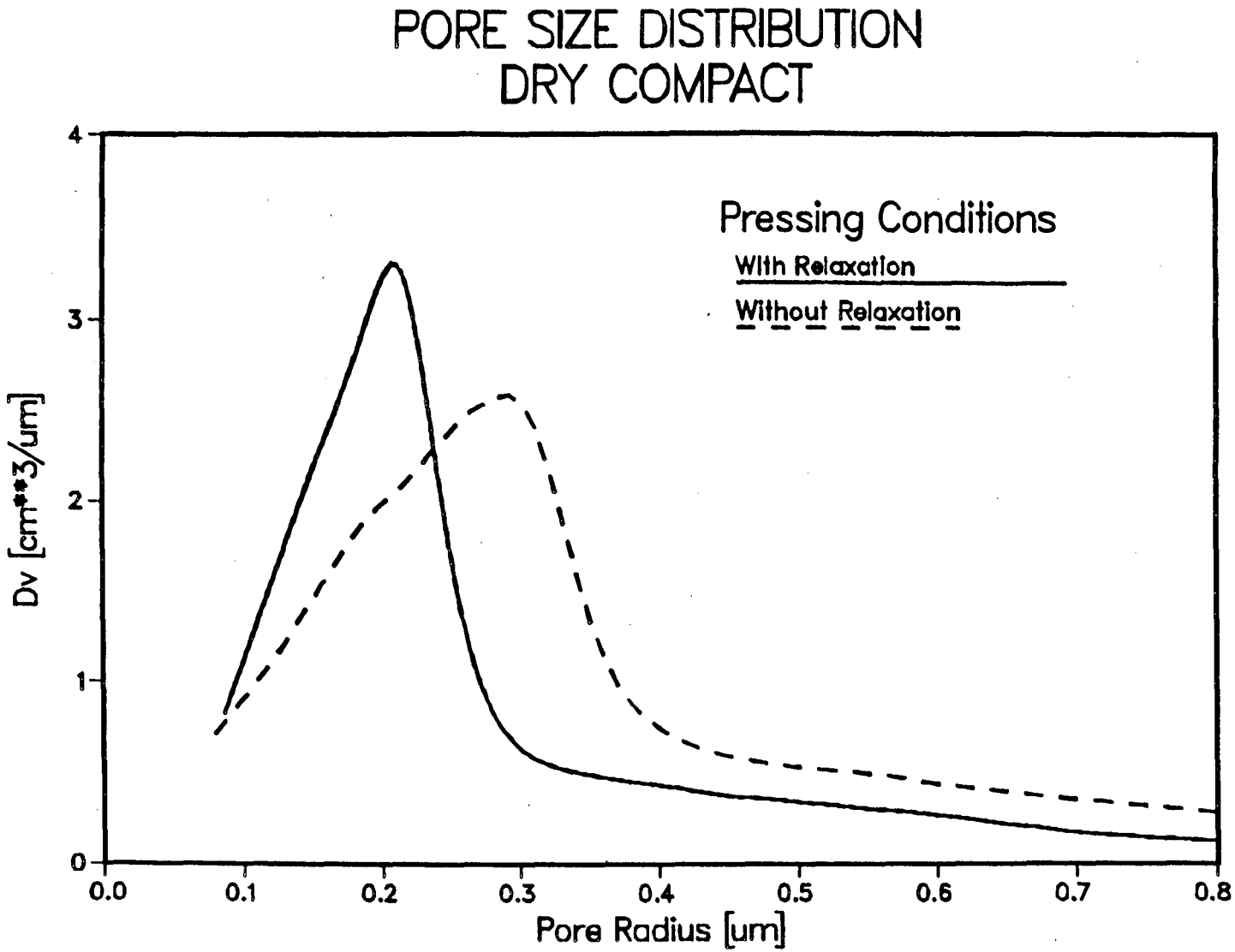

Fig. 6

XBL 857-3098

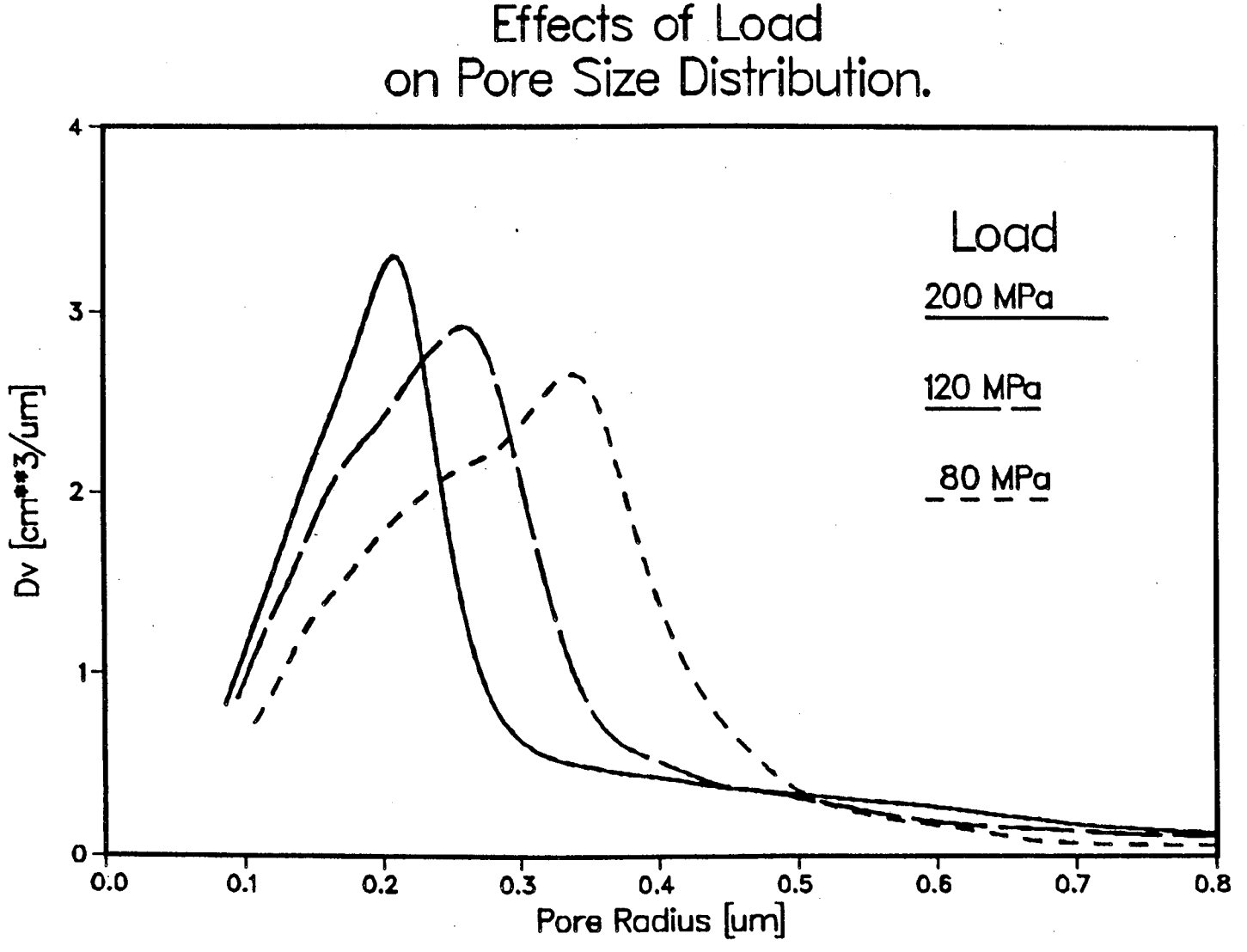

Fig. 7

XBL 857-3093

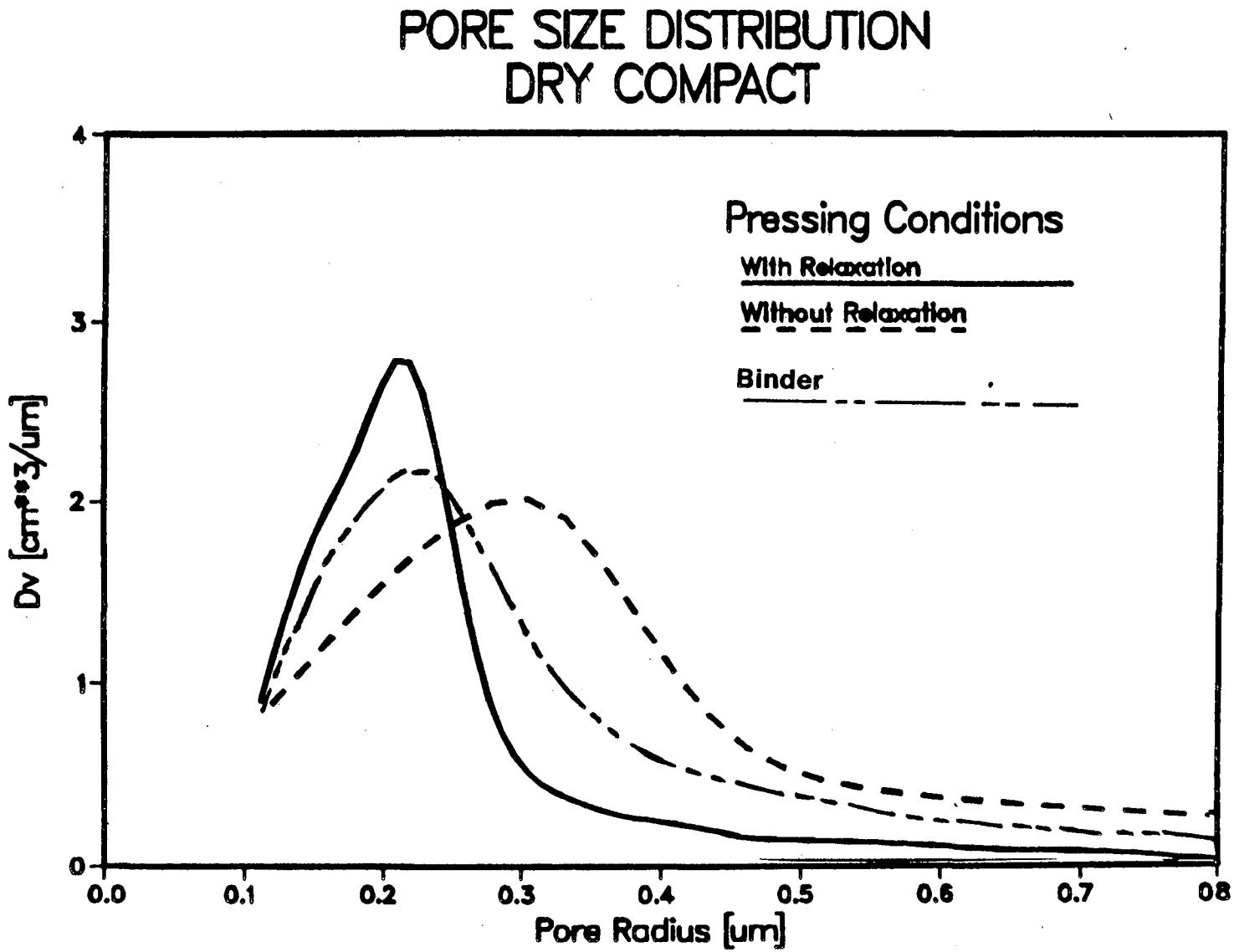

Fig. 8

XBL 857-3103

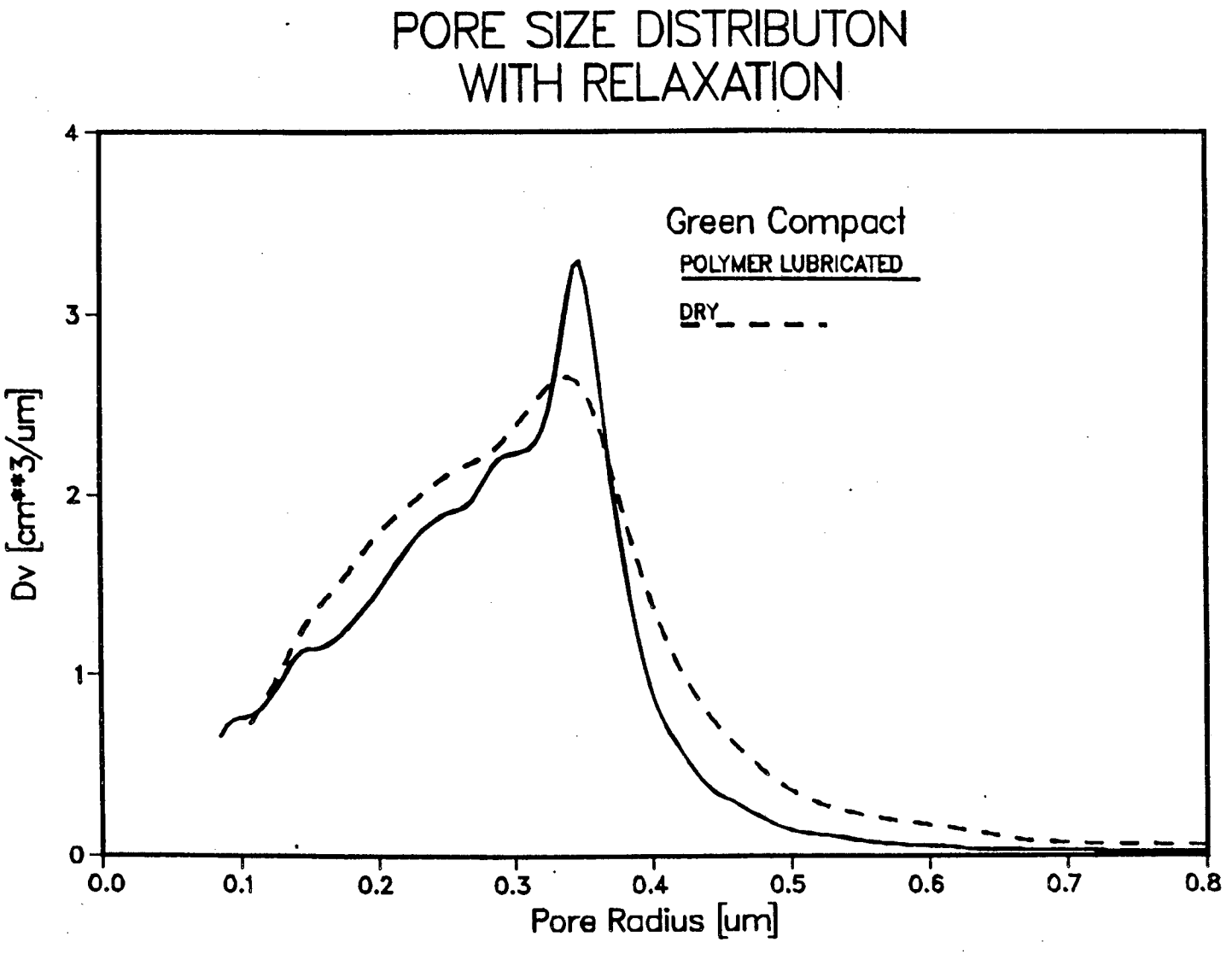

Fig. 9

XBL 857-3096

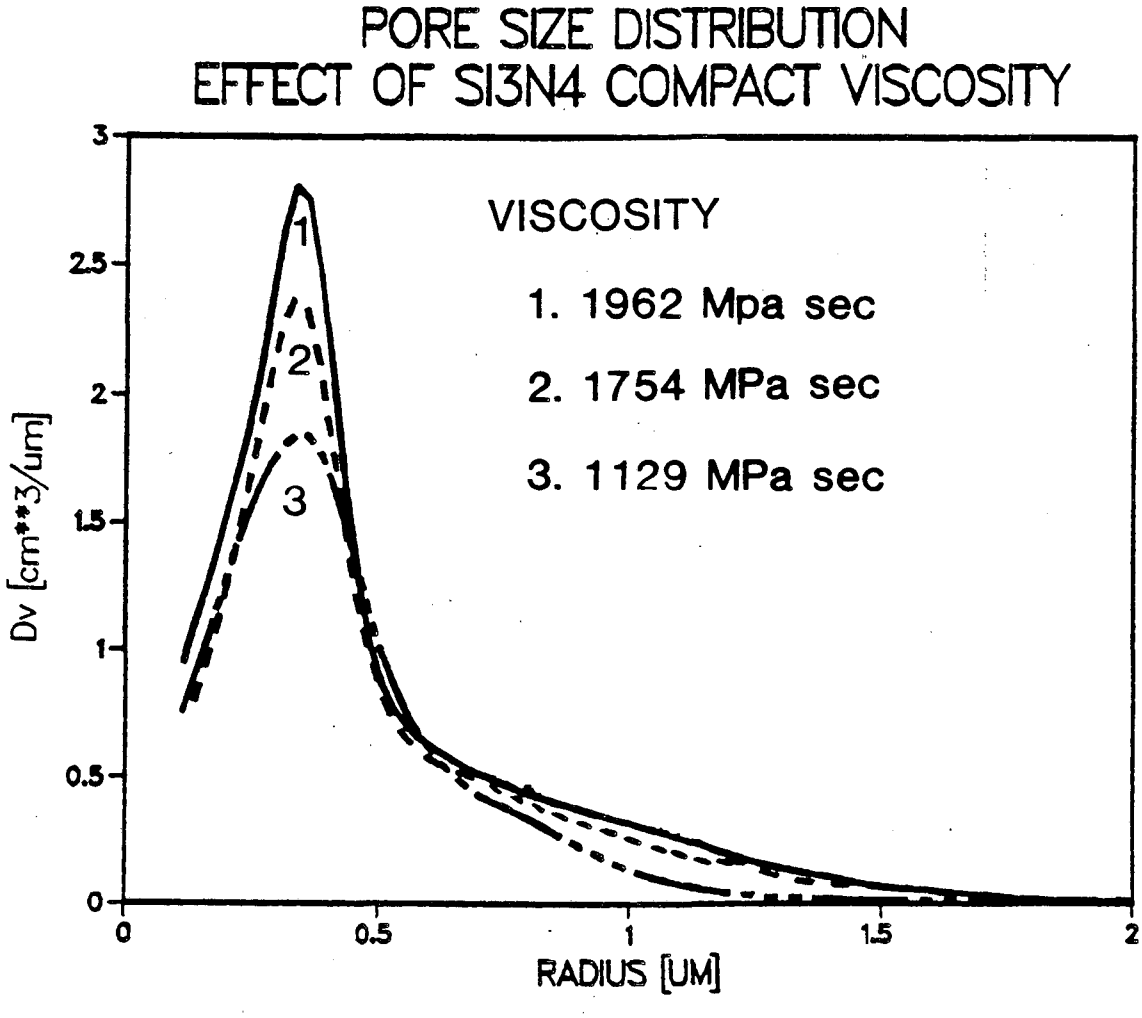

Fig. 10

XBL 858-3666

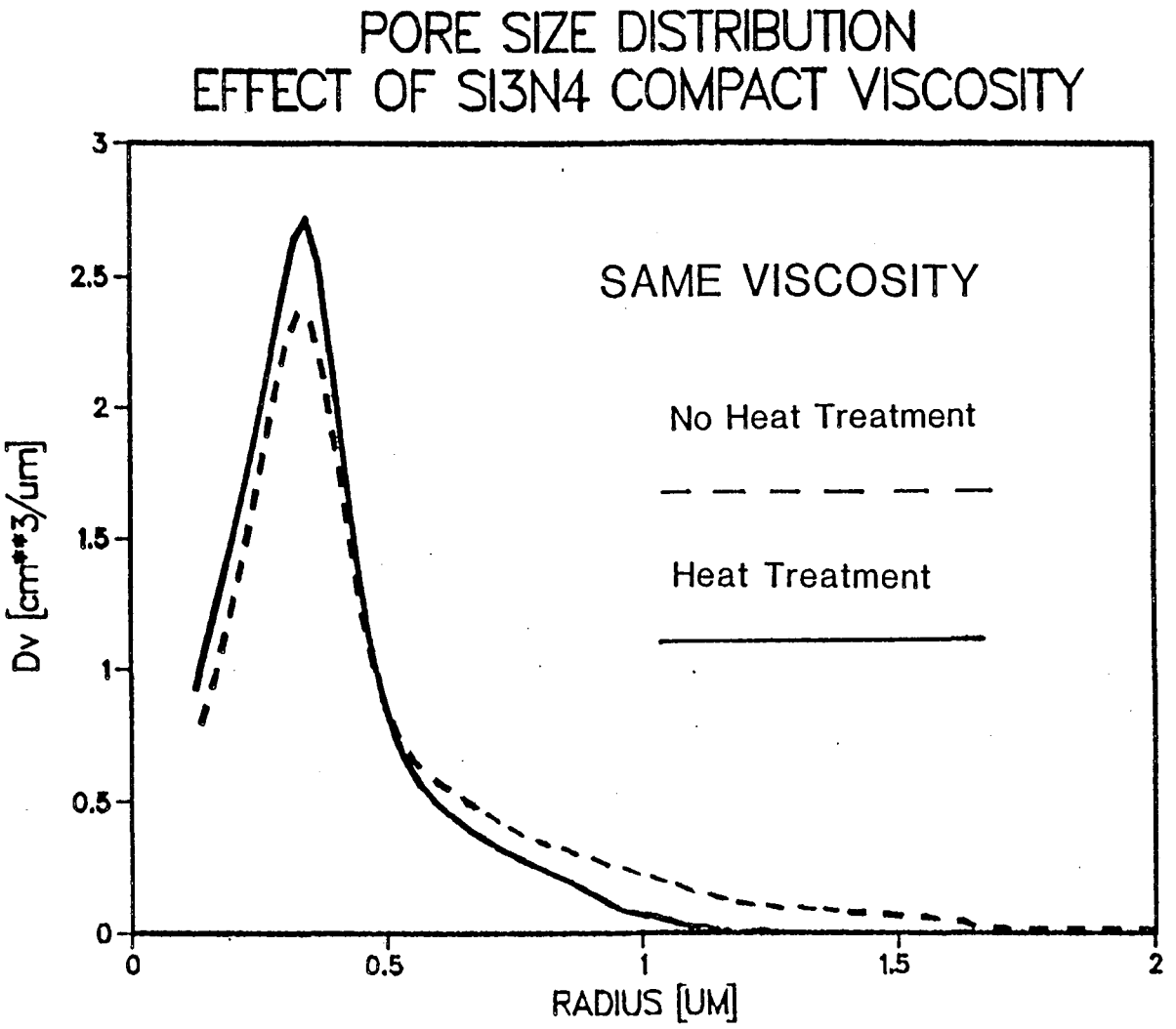

Fig. 11

XBL 857-3092

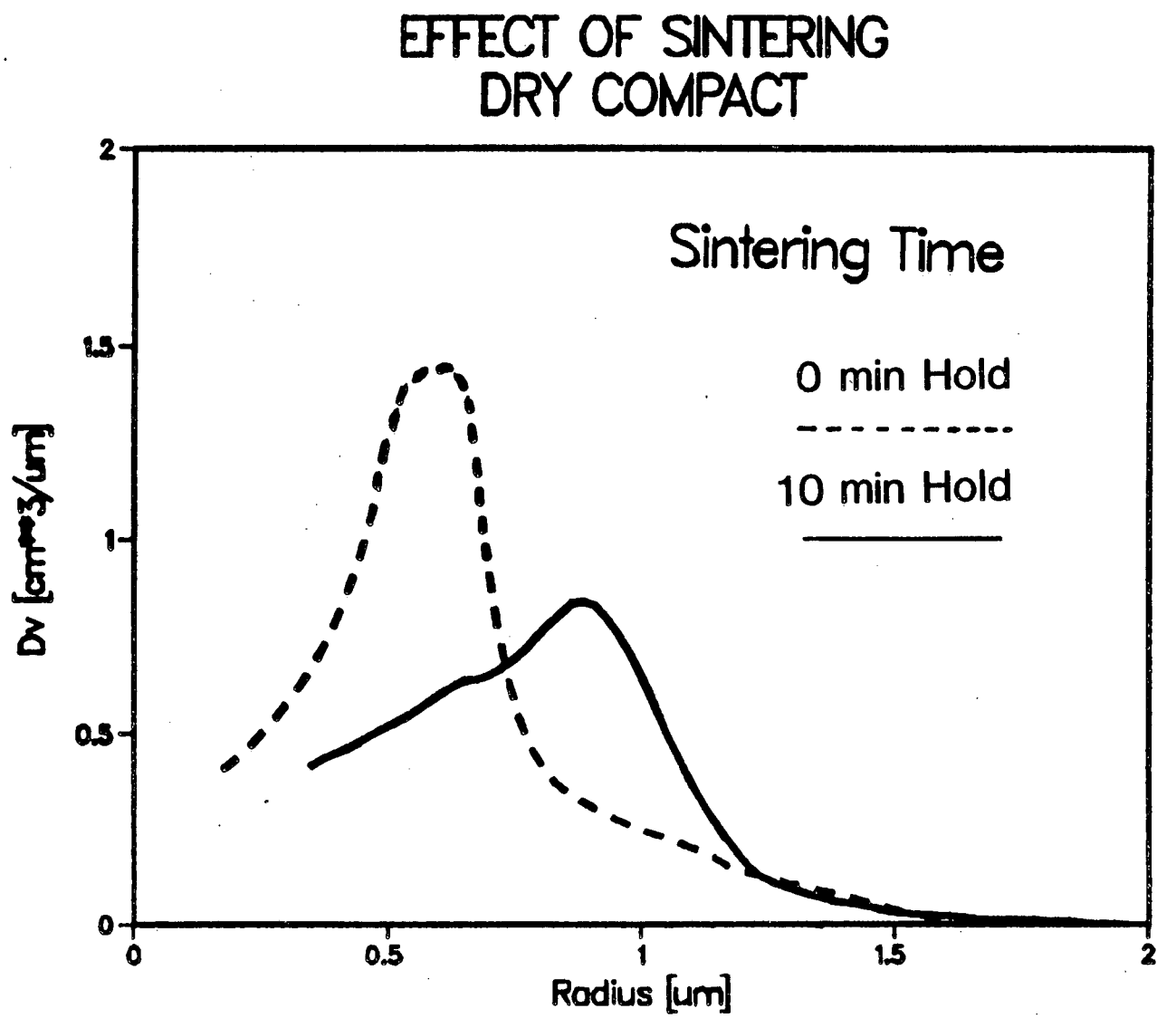

Fig. 12

XBL 857-3104

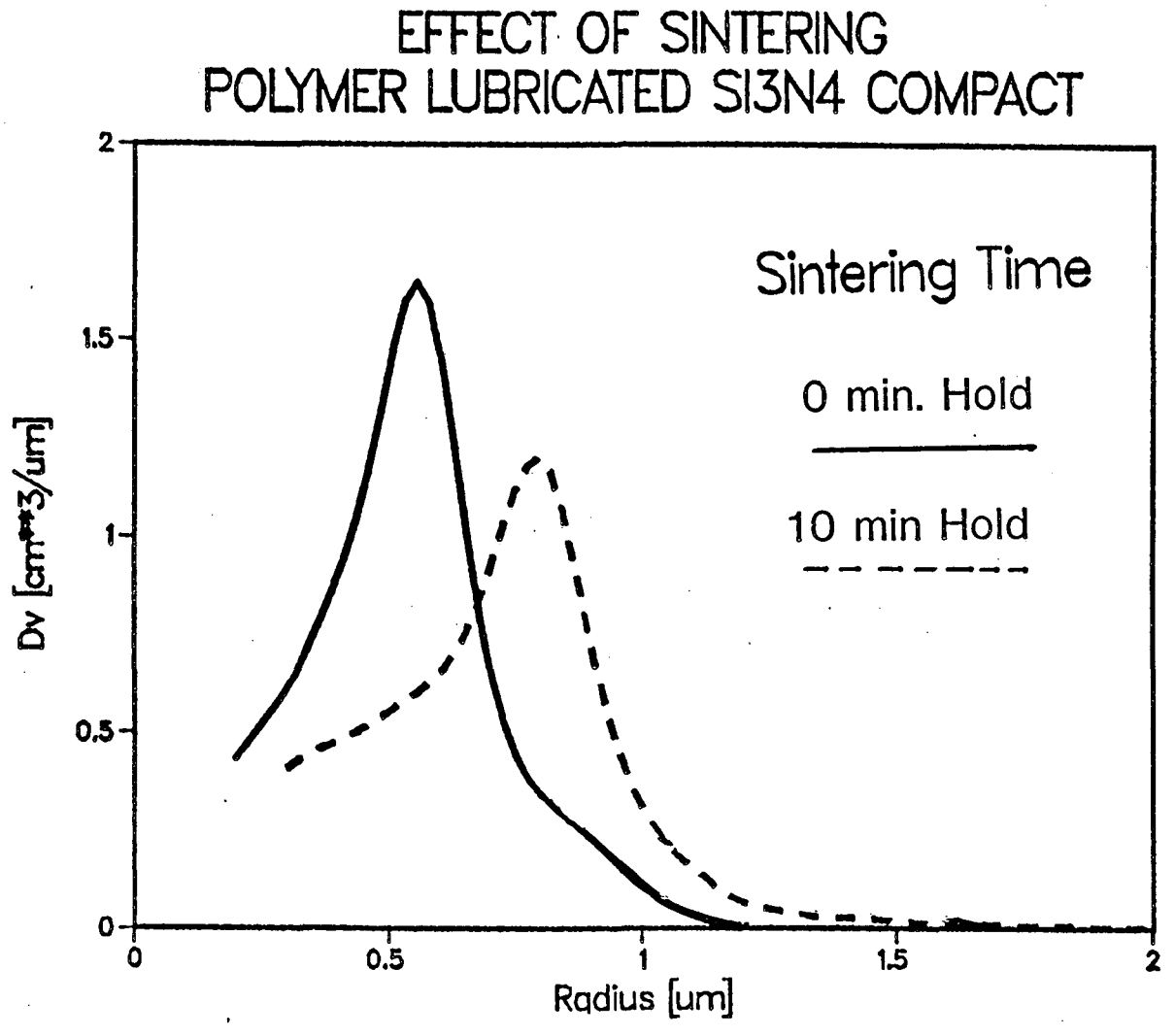

Fig. 13

XBL 857-3095

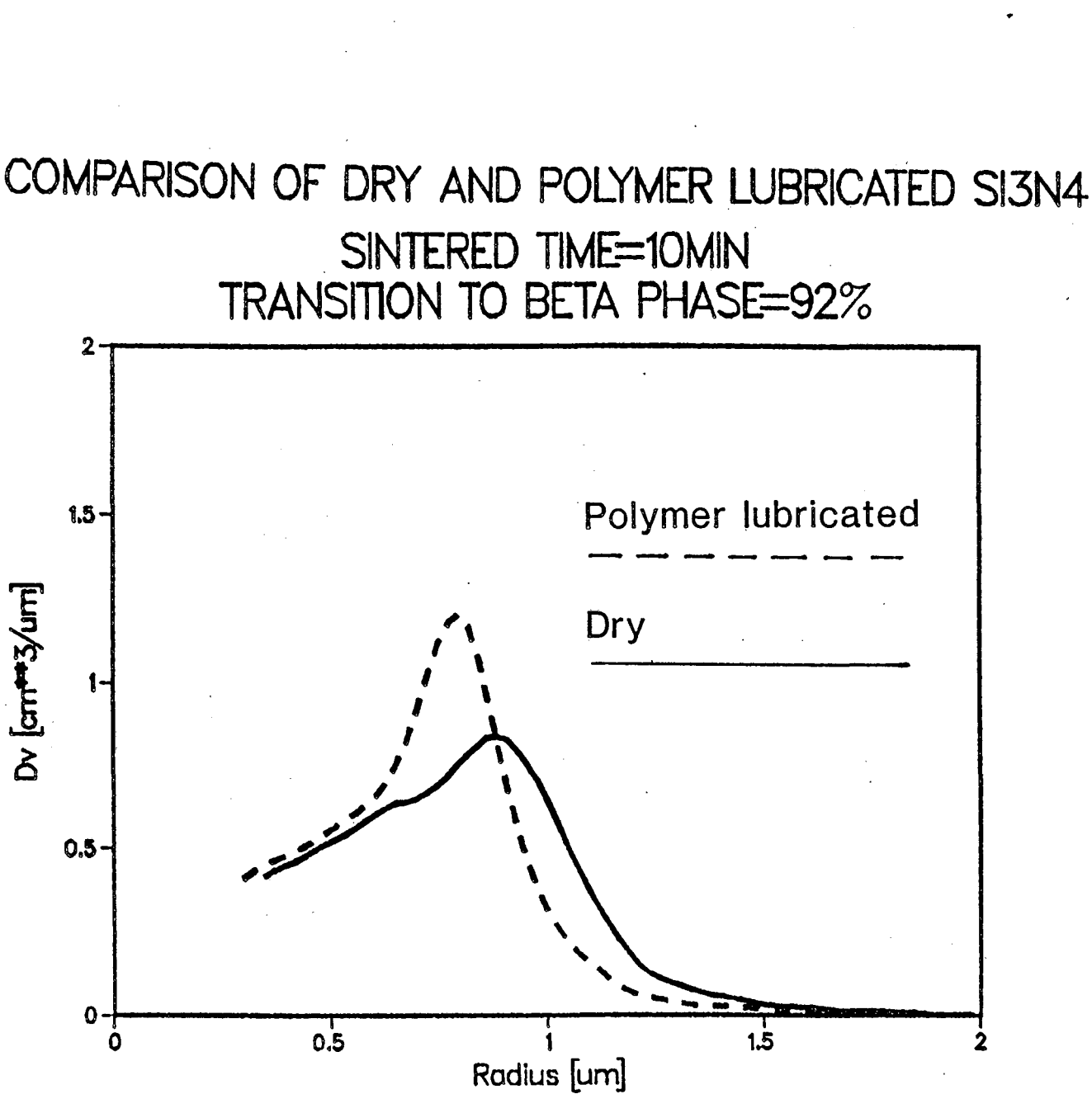

Fig. 14

XBL 857-3094

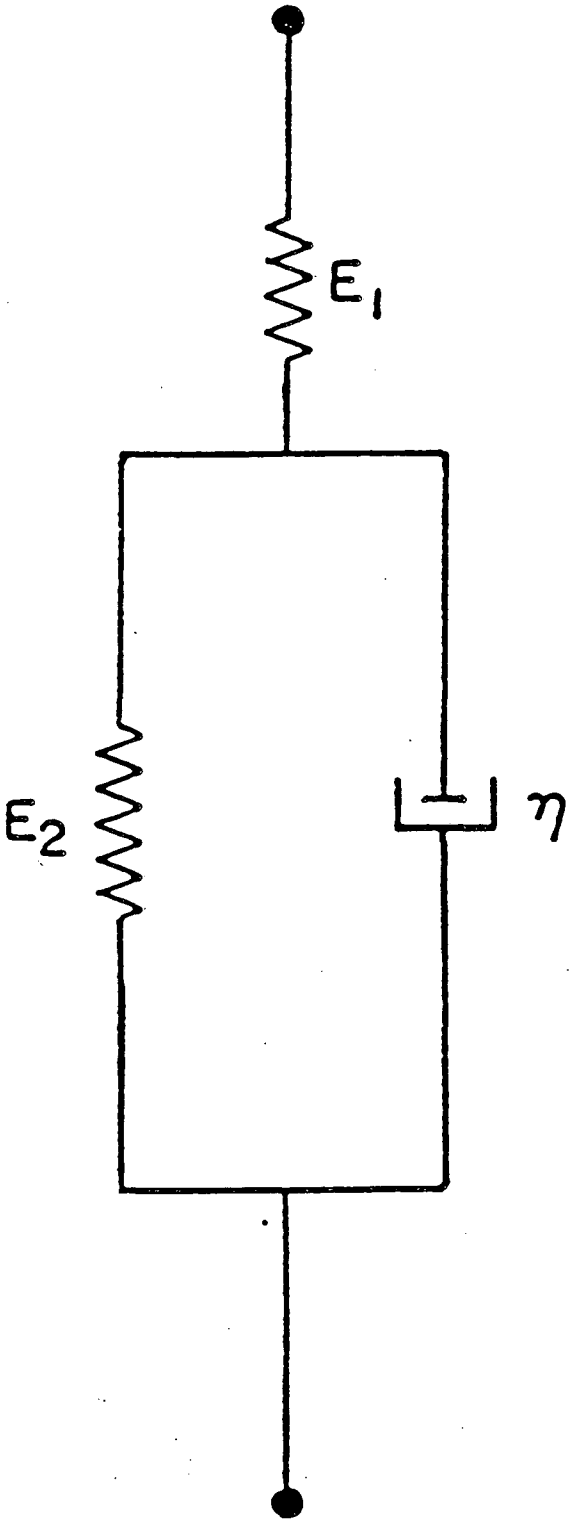

Fig. 15

XBL 857-3105

TABLE I

Preparation Method (Type of Reaction)		Reaction of SiO_2-N_2 in presence of C (solid-gas)	Nitridation of Si metal powder (solid-gas)		Vapor phase reaction of $SiCl_4$-NH_3 (gas-gas)	
Manufacturer		Toshiba	Starck		GTE	
Powder grade		n/a	H1	LC12	SN402	SN502
% alpha Si_3N_4		95	92	94	-	56
% beta Si_3N_4		3	4	3	-	3
% amorphous		-	-	-	92	39
% SiO_2		5.6	2.4	3.0	7.5	1.9
Specific surface(BET)	m^2/g	5	9	23	11	4
Grain size	µm	0.4-1.5	0.1-3	0.1-1	0.1-1.5	0.2-2
Apparent density	g/cm^3	0.20	0.37	0.40	0.18	0.1
Tap density	g/cm^3	0.43	0.64	0.87	0.26	0.26
% metallic impurities		0.1	0.1	0.1	0.2	0.1
% non-metallic impurities		4.1	1.7	1.7	4.6	1.1
morphology		partly aggregated uniform globular	discrete globular to irregular	discrete uniform globular	discrete uniform globular	aggregated globular and whiskers

TABLE II
SUMMARY OF VISCOSITY MEASUREMENT (Appendix B)

Compact[+]	Viscosity (Powder/polymer after Compaction)
a. 1g/5cc	1962 MPa sec
b. 1g/10cc	1754 MPa sec
c. 1g/15cc	1129 MPa sec
d. 1g/5cc (Heat Treated)	594 MPa sec

[+] 1g of polystyrene mixed with 5, 10, or 15 cc of chloroform as viscous lubricant binder. Powder quantity was fixed at 0.75g.

LAWRENCE BERKELEY LABORATORY
TECHNICAL INFORMATION DEPARTMENT
UNIVERSITY OF CALIFORNIA
BERKELEY, CALIFORNIA 94720